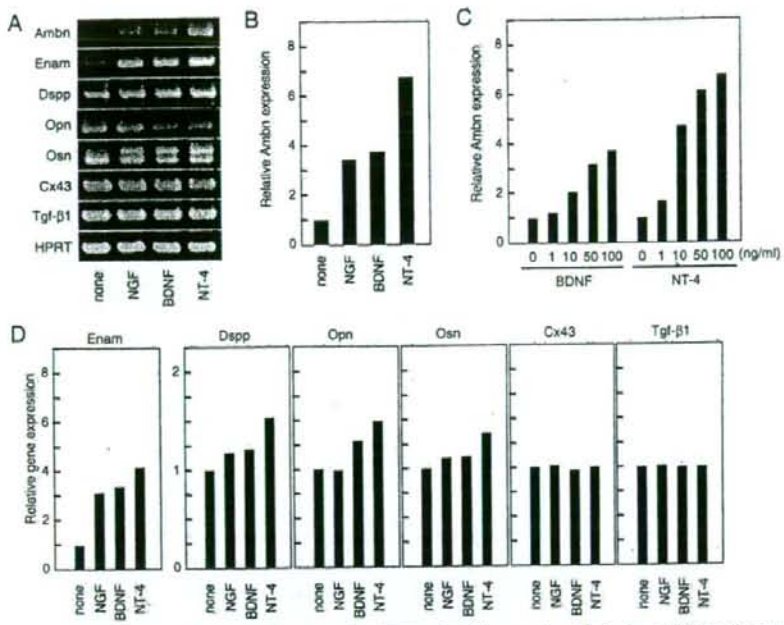

FIGURE 3. **Expression of tooth marker genes in HAT-7 cells with neurotrophic factors.** HAT-7 cells were cultured with 100 ng/ml NGF, BDNF, or NT-4 for 48 h. Total mRNA was analyzed for the expression of various genes by semiquantitative RT-PCR. Ambn, Enam, dentin sialophosphoprotein (*Dspp*), osteopontin (*Opn*), osteonectin (*Osn*), connexin 43 (*Cx43*), and transforming growth factor-β1 (*Tgf-β1*) (*A*). Hprt was used as an internal control. The level of gene expression in the absence of growth factors was set at 1 for comparison (*B* and *D*). HAT-7 cells were stimulated with various amounts of NT-4 and BDNF for 48 h. Hprt expression showed no significant difference between each culture. The level of Ambn expression in cells without factors was set at 1 for comparison (*C*).

Amel was also induced by NT-4 (data not shown). This effect was similar on all of the various amelogenin isoforms. The expression level of Ambn induced by NT-4 was higher than those by NGF or BDNF (Fig. 3*B*). The induction of Ambn expression by BDNF or NT-4 was dose-dependent (Fig. 3*C*), with the higher level by NT-4. The expression of gap junctional proteins (Gja1) and transforming growth factor-β1 was the same between the control and neurotrophic factor-treated cells (Fig. 3*D*). These results indicate that NT-4 induces enamel matrix genes and promotes ameloblast differentiation.

NT-4 and BDNF Induce Expression of Their Receptor but Not p75—Since the expression level of *TrkB* receptors is important for NT-4 signaling, we examined their expression in HAT-7 cells with or without NT-4 by RT-PCR (supplemental Fig. 1). We found that *TrkB-FL*, *TrkB-T1*, and *TrkB-T2* were highly induced by NT-4 and BDNF. NGF also induced the expression of *TrkB-FL* and *TrkB-T1*, but not *TrkB-T2* (supplemental Fig. 1, *A* and *B*).

Overexpression of TrkB-FL Enhances NT-4-mediated Ambn Induction—NT-4 induced expression of Ambn, *TrkB-FL*, and truncated *TrkB*. However, it is not clear which receptor is active for NT-4-mediated Ambn induction. To assess this question, we stably transfected HAT-7 cells with the *TrkB-FL* or *TrkB-T1* expression construct, cultured them with NT-4, and analyzed Ambn expression by RT-PCR. Ambn expression was induced by NT-4 in untransfected cells as shown in Figs. 3, *A* and *B*, and 4*A*. This NT-4-mediated Ambn induction was increased in *TrkB-FL*-transfected cells (Fig. 4, *A* and *B*). The basal level of Ambn expression was also higher in the transfected cells than in untransfected cells. However, in *TrkB-T1*-transfected cells, NT-4-mediated Ambn induction was inhibited (Fig. 4, *A* and *B*). Similar results were obtained from immunohistological analysis using Ambn antibody (data not shown). Furthermore, Ambn expression induced by NT-4 in *TrkB-FL* transfectants was completely inhibited by K252a, a *Trk* tyrosine kinase inhibitor (Fig. 4, *C* and *D*). These results indicate that the induction of Ambn by NT-4 is regulated via *TrkB-FL* but not by truncated *TrkB-T1*.

NT-4 Activates ERK1/2—In neuronal cells, NT-4 induces phosphorylation of *TrkB* and activates the Ras-MEK-ERK1/2 pathway (8). To analyze NT-4 signaling in the dental epithelium, we performed Western blotting using anti-phospho-specific ERK1/2 (MAPK) antibody. Phosphorylation of ERK1/2 was observed at 5 min after stimulation with NT-4 and then disappeared after 30 min (Fig. 5*A*). Further, the level of phosphorylation of ERK2 was higher than that of ERK1 (Fig. 5*B*). Next, we examined the ERK1/2 phosphorylation level in *TrkB*-transfected HAT-7 cells in the presence of NT-4 (Fig. 6, *A* and *B*). *TrkB-FL*-transfected cells showed strong activation of ERK1/2 at 5 min after the NT-4 treatment. However, the activation of ERK1/2 was not observed in *TrkB-T1*-transfected cells. These results indicate that full-length *TrkB-FL* is a major *TrkB* receptor for NT-4 signaling, and truncated *TrkB-T1* acts as a dominant negative factor for dental epithelial cells.

Trk Inhibitor K252a Inhibits Ambn Expression—NT-4 binds to *TrkB* and the low affinity receptor p75 and transduces downstream cellular signaling (8). To identify the signaling pathway involved in Ambn expression, we treated HAT-7 cells with the *Trk* inhibitor K252a or p75 inhibitor TAT-pep5 prior to stimulation with NT-4 (Fig. 7, *A* and *B*). NT-4-medaited induction of Ambn was significantly inhibited by K252a and TAT-pep5. Moreover, the induction of *TrkB* receptors by NT-4 was also inhibited by K252a and TAT-pep5. The inhibitory effect by K252a was higher than that by TAT-pep5. The MEK inhibitor PD98059 inhibited phosphorylation of neurotrophic factor-induced ERK1/2, and PD98059 treatment also inhibited the NT-4-mediated Ambn induction in HAT-7 cells (data not shown). These results suggest that ligand-induced activation of *TrkB* and p75 is important for the expression of Ambn, *TrkB-FL*, and *TrkB-T1*.

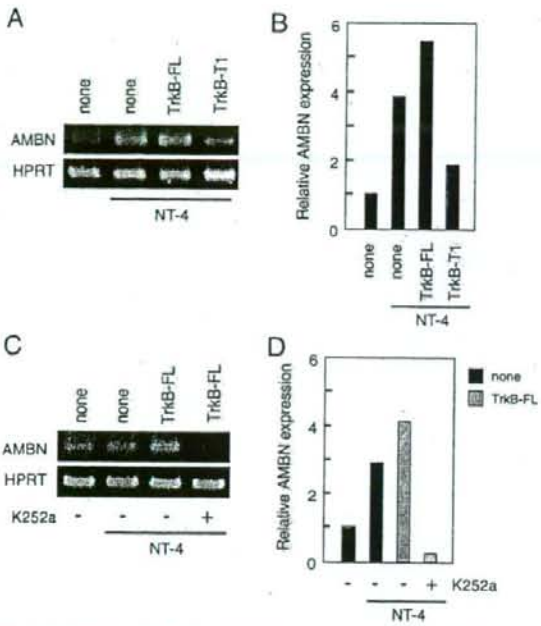

FIGURE 4. **Increase in NT-4-mediated Ambn induction in HAT-7 cells by overexpressing *TrkB-FL*.** The expression constructs for *TrkB-FL* and *TrkB-T1* receptors were stably transfected into HAT-7 cells. The pooled transfected cells were treated with NT-4 for 48 h. Ambn expression was analyzed using RT-PCR (*A*). The level of Ambn expression in the control cells without NT-4 was set at 1 for comparison (*B*). The *TrkB-FL* transfectant cells were cultured with or without K252a in the presence of NT-4 for 48 h and then analyzed for the expression of Ambn (*C*). The level of gene expression in the control cells without NT-4 was set at 1 for comparison (*D*).

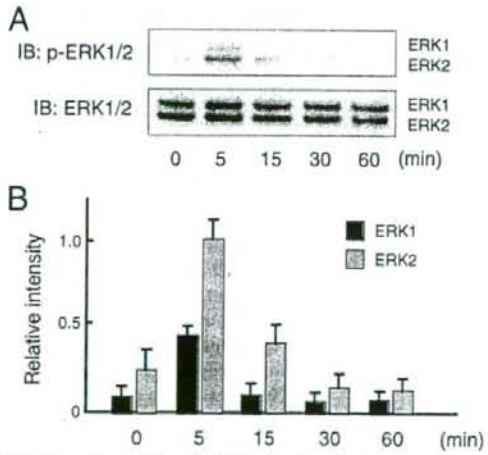

FIGURE 5. **Phosphorylation of ERK1/2 stimulated by NT-4.** The time course of phosphorylation of ERK1/2 after NT-4 treatment was analyzed by Western blotting (*IB*) using the anti-phospho-MAPK antibody (*A*). For the quantitations of *A*, the relative intensity of phosphorylated ERK1/2 (*p-ERK1/2*) in HAT-7 cells after 5 min was set at 1 for comparison (*B*).

NT-4 Null Mice Develop a Thin Enamel Layer and Have Reduced Ambn Expression—We demonstrated that NT-4 promoted epithelia cell differentiation in culture. To examine *in vivo* function of NT-4 in tooth development, we analyzed molars of NT-4 null mice (Fig. 8). NT-4 expression was completely absent in tooth germs of P1, P3, and P7 mice (supplemental Fig. 3). The expression of *TrkB* in NT-4 null tooth germs was similar to that of heterozygotes and wild-type mice (data not shown). We found that P3 molars had a thinner enamel matrix layer than control, whereas there was no significant difference in the predentin and dentin (Fig. 8, *A* and *B*). The size, shape, and polarization of ameloblasts in the mutant molars were normal as compared with those of the heterozygotes. Furthermore, Ambn expression in NT-4 null tooth germs was reduced as compared with that in heterozygotes (Fig. 8, *C* and *D*). These results suggest that NT-4 regulates Ambn expression and enamel layer formation.

DISCUSSION

Our results show that NT-4 regulates dental epithelial cell differentiation and enamel matrix gene expression via *TrkB-FL* but not via truncated *TrkB* forms. NT-4 inhibited cell proliferation and also induced enamel matrix genes, such as Ambn in dental epithelial cells. NT-4-deficient teeth resulted in a thin enamel layer during the initial stage of amelogenesis. Our findings are the first to show that a neurotrophic factor plays an important role in tooth development.

The functional roles of NT-4 and its receptors have been reported mainly in neuronal tissues. Complete ablation of p75 in mice causes defects in both the nervous and vascular systems (23). Those animals displayed sensory and sympathetic defects, thus demonstrating that the p75 receptor is required for proper neuronal development. *TrkB* mutants display severe phenotypes that result in the death of most mutant mice in the first postnatal week because of their inability to feed (24), whereas NT-4 knock-out mice are viable and fertile but have a 50% loss of neurons in the nodose-petrosal and geniculate ganglia (25, 26). BDNF knock-out mice are characterized by selective sensory disorders and have a reduced number of neurons in sensory ganglia; they do not survive longer than 3–4 weeks after birth (27, 28). Although NT-4 and BDNF use *TrkB* as a receptor, phenotypes of *TrkB*, NT-4, and BDNF knock-out mice differ each other. Thus, it is suggested that NT-4 has a different expression pattern and function from that of BDNF. In fact, NT-4, but not BDNF, is expressed in the inner dental epithelium. During tooth germ development, NGF is expressed in the dental mesenchyme but not in the dental epithelium (20). In contrast, BDNF is found in the dental mesenchyme in the human tooth germ but not in that of mice. In the present study, both NGF and BDNF induced expression of the ameloblast markers, Ambn and Enam, and NT-4 receptors, *TrkB-FL* and *TrkB-T1*. NGF and BDNF may be important for mesenchymal and epithelial interactions. NT-4 was expressed mostly in dental epithelia in tooth germs and has been detected in both dental epithelial and mesenchymal cell lines, suggesting that it functions in an autocrine manner in dental epithelium. We found that p75 was expressed in an undifferentiated dental epithelial cell line but was not detectable in the tooth germ. It was

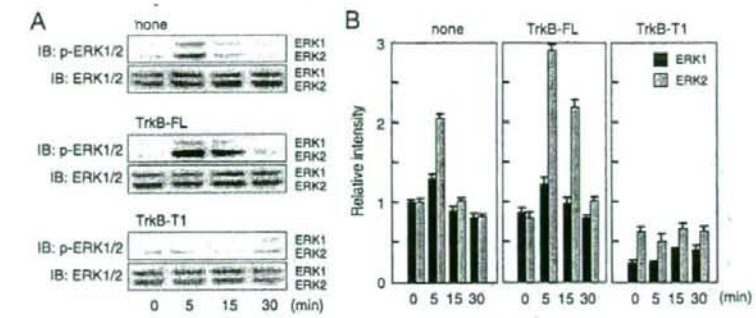

FIGURE 6. **Increase in phosphorylation of ERK1/2 in *TrkB-FL* transfectant cells by NT-4.** The time course of phosphorylation of ERK1/2 in *TrkB-FL*- and *T1*-transfected HAT-7 cells after treatment with NT-4 was analyzed by Western blotting (*IB*) using the anti-phospho-MAPK antibody (*A*). The Western blots with anti-MAPK showed equivalent amounts of total ERK proteins in each *lane*. The relative intensity of p-ERK1 in the control cells at 0 min was set at 1 for comparison (*B*).

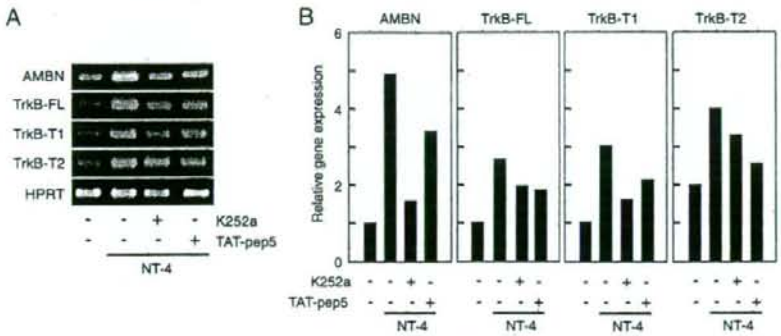

FIGURE 7. **Inhibition of NT-4-mediated induction of Ambn and *TrkBs* by K252a and TAT-pep5.** HAT-7 cells were treated with NT-4 in the presence of K252a or TAT-pep5. The expressions of Ambn, *TrkB-FL*, *TrkB-T1*, and *TrkB-T2* were analyzed by semiquantitative RT-PCR with specific primer sets (*A*). The level of gene expression in the control cells without NT-4 was set at 1 for comparison (*B*).

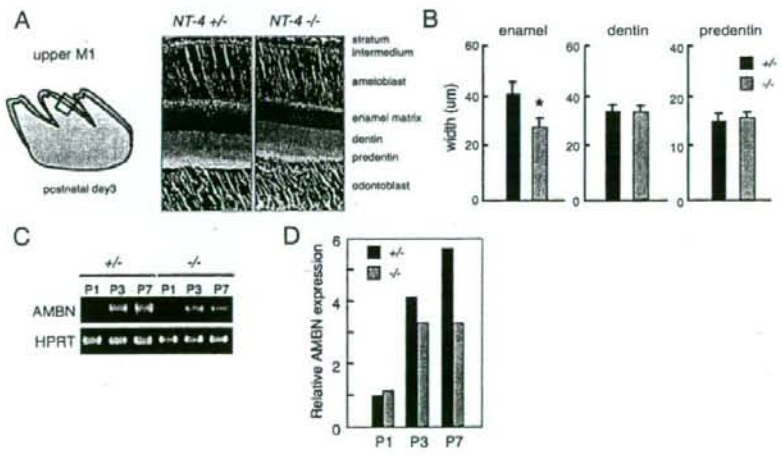

FIGURE 8. **Decrease in the enamel matrix width and expression of Ambn in NT-4 null mice.** Hematoxylin and eosin staining of P3 mouse molars were performed (*A*). The widths of the enamel matrix, dentin, and predentin were measured (*B*). Developing molars from heterozygote and mutant mice were dissected from P1, P3, and P7 mice, and total mRNA was prepared. The expression of Ambn was analyzed by semiquantitative RT-PCR with an Ambn primer set (*C*). The level of Ambn expression in P1 heterozygote mice was set at 1 for comparison (*D*).

reported that in incisors, p75 is expressed in the inner dental epithelium but is completely absent in differentiated ameloblasts (6). Further, the possibility of epithelial-mesenchymal communication within the intact tooth germ, whereas there is complete absence of those effects in the individual cells cultures, may be at the root of the differences of p75 expression between tooth germ and dental epithelial cell cultures. Moreover, p75 expression was not changed after stimulation with neurotrophins, whereas the p75 inhibitor TAT-pep5 was less effective on the expression of Ambn than *Trk* inhibitor K252a. These results suggest that p75 may not be important for the expression of Ambn in ameloblasts.

Truncated *TrkB* receptors have dominant inhibitory effects on BDNF and presynaptic signaling for BDNF-induced synaptic potentiation in cultured hippocampal neurons (29, 30). Truncated *TrkB-T1* mediates neurotrophin-evoked calcium signaling in glia cells (31) and plays a direct signaling role in mediating inositol-1,4,5-trisphoshate-dependent calcium release. In developing teeth, *TrkB-T1*, but not *TrkB-FL* or *TrkB-T2*, is detected by *in situ* hybridization (32). In the present study, all types of *TrkB* were detected in P3 tooth germ epithelia and a dental epithelial cell line. This discrepancy of *TrkB* expression may have occurred because of different detection efficiencies of the methods used. Although both *TrkB-FL* and truncated *TrkB* were induced by NT-4, overexpression of *TrkB-FL* enhanced the expression of Ambn, but *TrkB-T1* had a dominant negative effect on NT-4-induced Ambn expression. In NT-4-null mice, the expression of *TrkB-T1* and *-T2* was not changed from normal levels. These results suggest that truncated *TrkB* does not have an inhibitory effect on Ambn expression induced by NT-4.

Ambn plays an important role in maintaining the differentiation state of ameloblasts, serves as a cell

adhesion molecule, and inhibits the proliferation of the dental epithelium (6). A deficiency of Ambn causes severe enamel hypoplasia, accelerates proliferation of the dental epithelium, and decreases the expression of amelogenin. The Ambn promoter functions in a cell type-specific manner and contains cis-acting elements that function to enhance and suppress transcription (33). The transcription factor Runx2, known as an essential factor for transcription of mineralized tissue genes, is also required for Ambn transcription (33). Site-directed mutagenesis of the Runx2-binding site in the Ambn promoter decreases Ambn promoter activity in the dental epithelium (33). Sp3, a member of the Sp family of transcription factors, is ubiquitously expressed and present in ameloblasts at the presecretory and secretory stages but not the maturation stage. Sp3-deficient embryos show growth retardation and invariably die at birth of respiratory failure (34), and both endochondral and intramembranous ossification are impaired (35). These mice also have a pronounced defect in late tooth formation. In Sp3-null mice, the enamel and dentin layers of teeth are impaired due to the lack of ameloblast-specific gene products, including Ambn. These results indicate that Runx2 and Sp3 are necessary for the expression of Ambn. Our data suggest that NT-4 is also required for a high level of the expression of Ambn. We showed that NT-4 did not have an effect on the expression of Runx2 in the dental epithelium (supplemental Fig. 2). Further, K252a treatment also did not cause any differences in Runx2 or Sp3 expressions. Thus, neurotrophic factor signaling is not required to regulate the expression of Runx2 and Sp3. The ERK-MAPK pathway provides a major link between the cell surface and nucleus to control proliferation and differentiation. The inhibition of MAPK signaling blocks osteoblast-specific gene expression in mature osteoblasts, whereas a constitutive active form of the MAPK intermediate, MEK1, is stimulatory (36). Runx2 is required for cells to respond to MAPK *in vitro* (37). FGF2 induces osteocalcin expression through MAPK activation in osteoblast cell line and bone marrow stromal cells (40). We demonstrated that in the dental epithelium, ERK phosphorylation was induced by NT-4 and necessary for the phosphorylation of Ambn expression. In fact, the MEK inhibitor PD98059 inhibited ERK phosphorylation and Ambn expression in dental epithelium (data not shown). These results suggest that NT-4-*TrkB*-ERK signaling is important for Ambn expression and ameloblast differentiation.

REFERENCES

1. Thesleff, I., Vaahtokari, A., and Partanen, A. M. (1995) *Int. J. Dev. Biol.* **39,** 35–50
2. Zeichner-David, M., Diekwisch, T., Fincham, A., Lau, E., MacDougall, M., Moradian-Oldak, J., Simmer, J., Snead, M., and Slavkin, H. C. (1995) *Int. J. Dev. Biol.* **39,** 69–92
3. Fukumoto, S., and Yamada, Y. (2005) *Connect. Tissue Res.* **46,** 220–226
4. Fukumoto, S., Miner, J. H., Ida, H., Fukumoto, E., Yuasa, K., Miyazaki, H., Hoffman, M. P., and Yamada, Y. (2006) *J. Biol. Chem.* **281,** 5008–5016
5. Smith, C. E. (1998) *Crit. Rev. Oral Biol. Med.* **9,** 128–161
6. Fukumoto, S., Kiba, T., Hall, B., Iehara, N., Nakamura, T., Longenecker, G., Krebsbach, P. H., Nanci, A., Kulkarni, A. B., and Yamada, Y. (2004) *J. Cell Biol.* **167,** 973–983
7. Barbacid, M. (1994) *J. Neurobiol.* **25,** 1386–1403
8. Barbacid, M. (1995) *Curr. Opin. Cell Biol.* **7,** 148–155
9. Klein, R., Conway, D., Parada, L. F., and Barbacid, M. (1990) *Cell* **61,** 647–656
10. Middlemas, D. S., Lindberg, R. A., and Hunter, T. (1991) *Mol. Cell Biol.* **11,** 143–153
11. Tsoulfas, P., Soppet, D., Escandon, E., Tessarollo, L., Mendoza-Ramirez, J. L., Rosenthal, A., Nikolics, K., and Parada, L. F. (1993) *Neuron* **10,** 975–990
12. Valenzuela, D. M., Maisonpierre, P. C., Glass, D. J., Rojas, E., Nunez, L., Kong, Y., Gies, D. R., Stitt, T. N., Ip, N. Y., and Yancopoulos, G. D. (1993) *Neuron* **10,** 963–974
13. Verdi, J. M., Birren, S. J., Ibanez, C. F., Persson, H., Kaplan, D. R., Benedetti, M., Chao, M. V., and Anderson, D. J. (1994) *Neuron* **12,** 733–745
14. Mahadeo, D., Kaplan, L., Chao, M. V., and Hempstead, B. L. (1994) *J. Biol. Chem.* **269,** 6884–6891
15. Di Marco, E., Mathor, M., Bondanza, S., Cutuli, N., Marchisio, P. C., Cancedda, R., and De Luca, M. (1993) *J. Biol. Chem.* **268,** 22838–22846
16. Kalcheim, C., Carmeli, C., and Rosenthal, A. (1992) *Proc. Natl. Acad. Sci. U. S. A.* **89,** 1661–1665
17. Sariola, H., Saarma, M., Sainio, K., Arumae, U., Palgi, J., Vaahtokari, A., Thesleff, I., and Karavanov, A. (1991) *Science* **254,** 571–573
18. Rabizadeh, S., Oh, J., Zhong, L. T., Yang, J., Bitler, C. M., Butcher, L. L., and Bredesen, D. E. (1993) *Science* **261,** 345–348
19. Barrett, G. L., and Bartlett, P. F. (1994) *Proc. Natl. Acad. Sci. U. S. A.* **91,** 6501–6505
20. Luukko, K., Arumae, U., Karavanov, A., Moshnyakov, M., Sainio, K., Sariola, H., Saarma, M., and Thesleff, I. (1997) *Dev. Dyn.* **210,** 117–129
21. Nosrat, C. A., Fried, K., Lindskog, S., and Olson, L. (1997) *Cell Tissue Res.* **290,** 569–580
22. Yuasa, K., Fukumoto, S., Kamasaki, Y., Yamada, A., Fukumoto, E., Kanaoka, K., Saito, K., Harada, H., Arikawa-Hirasawa, E., Miyagoe-Suzuki, Y., Takeda, S., Okamoto, K., Kato, Y., and Fujiwara, T. (2004) *J. Biol. Chem.* **279,** 10286–10292
23. von Schack, D., Casademunt, E., Schweigreiter, R., Meyer, M., Bibel, M., and Dechant, G. (2001) *Nat. Neurosci.* **4,** 977–978
24. Klein, R., Smeyne, R. J., Wurst, W., Long, L. K., Auerbach, B. A., Joyner, A. L., and Barbacid, M. (1993) *Cell* **75,** 113–122
25. Conover, J. C., Erickson, J. T., Katz, D. M., Bianchi, L. M., Poueymirou, W. T., McClain, J., Pan, L., Helgren, M., Ip, N. Y., Boland, P., Friedman, B., Wiegand, S., Vejsada, R., Kato, A. C., Dechiara, T. H., and Yancopoulos, G. D. (1995) *Nature* **375,** 235–238
26. Liu, X., Ernfors, P., Wu, H., and Jaenisch, R. (1995) *Nature* **375,** 238–241
27. Ernfors, P., Lee, K. F., and Jaenisch, R. (1994) *Nature* **368,** 147–150
28. Korte, M., Carroll, P., Wolf, E., Brem, G., Thoenen, H., and Bonhoeffer, T. (1995) *Proc. Natl. Acad. Sci. U. S. A.* **92,** 8856–8860
29. Eide, F. F., Vining, E. R., Eide, B. L., Zang, K., Wang, X. Y., and Reichardt, L. F. (1996) *J. Neurosci.* **16,** 3123–3129
30. Li, Y. X., Xu, Y., Ju, D., Lester, H. A., Davidson, N., and Schuman, E. M. (1998) *Proc. Natl. Acad. Sci. U. S. A.* **95,** 10884–10889
31. Rose, C. R., Blum, R., Pichler, B., Lepier, A., Kafitz, K. W., and Konnerth, A. (2003) *Nature* **426,** 74–78
32. Luukko, K., Moshnyakov, M., Sainio, K., Saarma, M., Sariola, H., and Thesleff, I. (1996) *Dev. Dyn.* **206,** 87–99
33. Dhamija, S., and Krebsbach, P. H. (2001) *J. Biol. Chem.* **276,** 35159–35164
34. Bouwman, P., Gollner, H., Elsasser, H. P., Eckhoff, G., Karis, A., Grosveld, F., Philipsen, S., and Suske, G. (2000) *EMBO J.* **19,** 655–661
35. Gollner, H., Dani, C., Phillips, B., Philipsen, S., and Suske, G. (2001) *Mech. Dev.* **106,** 77–83
36. Xiao, G., Gopalakrishnan, R., Jiang, D., Reith, E., Benson, M. D., and Franceschi, R. T. (2002) *J. Bone Miner. Res.* **17,** 101–110
37. Ducy, P., Zhang, R., Geoffroy, V., Ridall, A. L., and Karsenty, G. (1997) *Cell* **89,** 747–754
38. Xiao, G., Jiang, D., Thomas, P., Benson, M. D., Guan, K., Karsenty, G., and Franceschi, R. T. (2000) *J. Biol. Chem.* **275,** 4453–4459
39. Franceschi, R. T., Xiao, G., Jiang, D., Gopalakrishnan, R., Yang, S., and Reith, E. (2003) *Connect. Tissue Res.* **44,** Suppl. 1, 109–116
40. Xiao, G., Jiang, D., Gopalakrishnan, R., and Franceschi, R. T. (2002) *J. Biol. Chem.* **277,** 36181–36187

Cell Tissue Res (2008) 331:447–459
DOI 10.1007/s00441-007-0532-1

REGULAR ARTICLE

Collagen type I matrix affects molecular and cellular behavior of purified porcine dental follicle cells

S. Tsuchiya · M. J. Honda · Y. Shinohara · M. Saito · M. Ueda

Received: 13 April 2007 / Accepted: 1 October 2007 / Published online: 13 November 2007

Abstract We investigated porcine dental follicle cells at the early crown-formation stage and examined the behavior of cells grown in a collagen type I (Col-I) matrix. Clone-porcine dental follicle cells (DFC-I) and controls, viz., dental follicle itself, nonclone-dental follicle cells, periodontal ligament cells (PDLC), and bone marrow stromal cells, were obtained from 6-month-old pigs. DFC-I showed a different gene expression pattern from controls by reverse-transcription polymerase chain reaction analysis. In addition, Col-I treatment enhanced DFC-I proliferation and increased their alkaline phosphatase activity compared with nontreated DFC-I. The expression of periostin, biglycan, and osteocalcin (OCN) in cells growing on collagen was upregulated, similar to the pattern seen in PDLC. DFC-I with and without Col-I treatment were combined with β-tricalcium phosphate particles and implanted into immunodeficient mice. Significant differences were found in the gene expression patterns of bone sialoprotein, OCN, and periostin in both treated and non-treated implants at 2 and/or 4 weeks. The results showed that Col-I induced the mineralization pathway in these cells. Hard tissue formation was observed in both implant types at 8 weeks. Our results suggest that Col-I facilitates the differentiation of DFC-I along the mineralization process.

Keywords Characterization · Clonal dental follicle cell · Collagen type I matrix · Dental follicle · Mineralization · Porcine

This work was supported in part by grants from the Japanese Ministry of Education, Culture, Sports, Science, and Technology (Kakenhi Kiban B 16390578 and Houga 18659592 to M.J.H.) and by the Hitachi Medical Corporation (Japan) and DENICS International (Japan).

S. Tsuchiya · M. J. Honda (✉) · Y. Shinohara · M. Ueda
Tooth Regeneration, The Division of Stem Cell Engineering,
The Institute of Medical Science, The University of Tokyo,
4-6-1 Shiroganedai, Minato-ku,
Tokyo 108-8639, Japan
e-mail: honda-m@ims.u-tokyo.ac.jp

S. Tsuchiya · M. Ueda
Department of Oral and Maxillofacial Surgery,
Nagoya University Postgraduate School of Medicine,
65 Tsurumacho, Showa-ku, Nagoya,
Aichi 466-8550, Japan

M. Saito
Department of Operative Dentistry and Endodontics,
Kanagawa Dental College,
82 Inaokacho, Yokosuka,
Kanagawa 238-8580, Japan

Introduction

The dental follicle (DF) is a loose, ectomesenchymally derived, connective tissue surrounding the enamel organ and the dental papilla of the developing tooth germ prior to eruption. The differentiation and function of dental follicle cells (DFC) are controlled by a network of regulatory molecules, including growth factors and cytokines (Thesleff and Mikkola 2002). Although the exact sequence of events and cells involved in the development of the periodontium is not established, previous studies have suggested that DFC populations also contain cementoblasts, periodontal ligament cells (PDLC), and osteoblast progenitor or precursor cells (Morsczeck et al. 2005; Palmer and Lumsden 1987; Ten Cate and Mills 1972; Ten Cate et al. 1971; Yoshikawa and Kollar 1981). Bovine DFC isolated from developing tooth germ at the root-forming stage can differentiate into cementoblasts on implantation into immunodeficient mice (Handa et al. 2002). However, the mechanisms regulating DFC differentiation remain poorly understood (Bartold et al. 1988; Diekwisch 2001; Saygin et al. 2000).

In the first part of this study, we isolated porcine DFC from third molars extracted at the early crown-formation stage. Using semiquantitative and real-time reverse-transcription polymerase chain reaction (sq-PCR and rt-PCR), we examined the expression of periodontal- and bone-related genes in these cells and compared them with the gene expressions of PDLC and bone marrow stromal cells (BMSC). The periodontal ligament (PDL) originates from DFC and contains heterogeneous cell populations (Lekic et al. 2001; Murakami et al. 2003). Recent findings suggest that PDLC have many osteoblast-like properties including the expression of bone-associated markers (Han and Amar 2003; Lekic et al. 2001; Marcopoulou et al. 2003; Ouyang et al. 2000; Pitaru et al. 2002). BMSC represent a population of nonhematopoietic marrow-derived cells, and their ability to differentiate into mesenchymal lineage includes osteoprogenitor cells (Bianco et al. 2001; Ducy et al. 1999). Recently, the skeletal site-specific characterization of orofacial BMSC was examined by Akintoye et al. (2006). Clone-porcine DFC (DFC-I) were derived from a single cell and were shown to adhere to a plastic substratum and to be clonogenic and competent to proliferate in vitro.

The extracellular matrix (ECM) relays complex signals from the cell microenvironment to direct proliferation and differentiation during tissue development. However, the role of the ECM and adhesion in DFC differentiation is poorly understood. BMSC undergo osteogenic differentiation in vitro when cultured on a collagen type I (Col-I) matrix (Mizuno and Kuboki 2001; Xiao et al. 1998). Moreover, Col-I also supports osteogenesis in BMSC and may induce differentiation in the absence of soluble osteoinductive factors (Klees et al. 2005; Salasznyk et al. 2004). Col-I is also a major organic component of the predentin-dentin matrix (Ruch 1998), and immature adult rat dental pulp cells strongly induces mRNA expression for dentin sialoprotein in Col-I gel cultures (Nakao et al. 2004). We have therefore hypothesized that Col-I might facilitate the differentiation of DFC. To test this, we cultured DFC on either dishes coated with purified Col-I (Col-I-d) or standard tissue-grade polystyrene dishes (P-d) and analyzed cell growth, alkaline phosphatase (ALPase) activity, and the expression of osteogenic differentiation-related marker genes. The gene expression patterns of Col-I-exposed DFC resembled that of PDLC. Periostin, biglycan, and osteocalcin (OCN) mRNAs were expressed, but bone sialoprotein (BSP) gene expression was absent.

As the final experiment in this study, we examined whether DFC-I could form hard tissue and assessed the effect of Col-I. The differentiated cells showed greater capacity to form hard tissue in vivo than the untreated cells. Our data presented herein provide new insights that Col-I affects the molecular and cellular behavior of purified porcine DFC.

Materials and methods

Isolation of highly purified DFC

As a preliminary experiment, mandibular third molar tooth buds were surgically removed from a 6-month-old porcine jaw and observed by histology and immunohistochemistry to establish the histogenesis (Fig. 1a–c). The DF and enamel organ were dissected as described previously (Wise et al. 1992). Briefly, the isolated DF was placed in 1% trypsin/1 mM EDTA (Invitrogen, Life Technologies, N.Y.) for 10 min at room temperature. The DF was separated from the dental enamel organ by microdissection and then incubated in 0.25% trypsin/1 mM EDTA (Invitrogen) for 10 min at 37°C to dissociate the porcine DFC. Approximately 3.0×10^6 DFC were obtained from one tooth bud. The DFC were cultured in Dulbecco's modified Eagle's medium (DMEM; Kohjin Bio, Saitama, Japan) containing 10% fetal bovine serum (Invitrogen), 2 mM penicillin-streptomycin-glutamine (Invitrogen), and 1 mM sodium pyruvate (Invitrogen) at 37°C in an atmosphere containing 5% CO_2. The medium was changed every 3 days until the third passage. DFC were then suspended at a density of 1 cell per 100 μl and seeded into three 96-well culture plates (Greiner Bio-one, Kremsmuenster, Austria). The cells were incubated for 2 weeks, and then six colonies (each from a single cell) were observed and subsequently subcultured. For the following experiments, the clonal cell populations that had the greatest proliferation rate were subcultured until the tenth passage (DFC-I; Fig. 2a,b). The DFC-I were grown to a maximum of 30 passages.

For comparison, cells were obtained from the PDL attached to the middle portion of the permanent incisor root and the alveolar bone surrounding the first molar tooth. These tissues were digested with 2 mg/ml collagenase (WAKO, Osaka, Japan), and the cells released were maintained as porcine PDLC (Fig. 2c,d) and porcine BMSC (Fig. 2e,f), respectively. The PDLC and BMSC at the third passages were used for following experiments.

Immunofluorescent staining

We tested whether the DFC-I were derived from the DF by using mesenchyme markers. DFC-I grown on coverslips were fixed with 4% paraformaldehyde for 10 min at room temperature and then treated with 0.5% Triton-X 100 (Sigma, St. Louis, Mo.) for 5 min to render them permeable. After the blocking of non-specific sites, the cells were treated for 60 min with sheep antibody to pig Col-I (gift from Dr. J. Sodek, University of Toronto, Canada) diluted 1:20 with phosphate-buffered saline (PBS), with mouse antibody to vimentin (NeoMarkers, Westinghouse, Calif.) diluted 1:1,000, or with an antibody to cytokeratin14 as a control

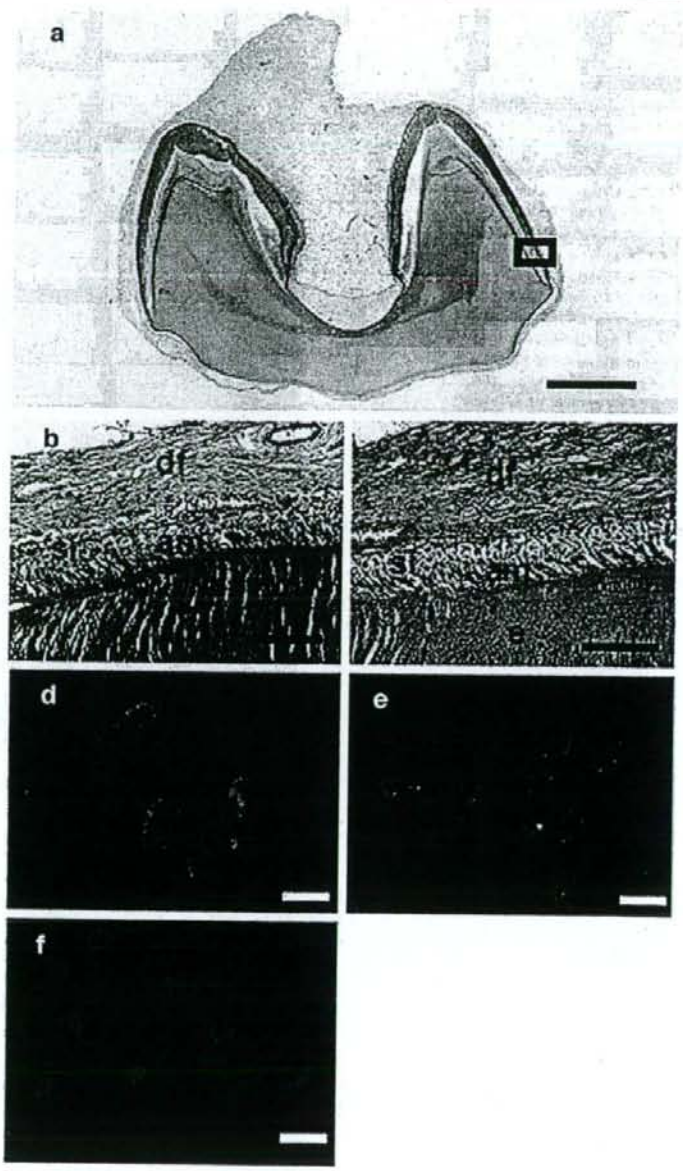

Fig. 1 Morphology of tissue and cells in porcine third molar at the crown-formation stage. **a** Morphology of third molar at the crown-formation stage shown by hematoxylin-eosin staining. Crown formation was well advanced at this stage. **b** Higher magnification of *boxed area* in **a** showing dental follicle (DF; *df*) distinguishable from the dental enamel organ and enamel (*e*). DF fibers were observed running close to the stratum intermedium (*si*) and contained fibroblastic cells (*am* ameloblast); hematoxylin-eosin staining. **c** Strong staining of collagen type I (Col-I) was identified in DF, but not in enamel or in enamel organ. **d**, **e** Immunofluorescence showed strong staining of all clone-porcine dental follicle cells (DFC-I) with specific antibody against vimentin and Col-I, respectively (*blue* DAPI nuclear staining). **f** DFC-I showed no staining with the specific antibody against cytokeratin14. *Bars* 1,000 μm (**a**), 100 μm (**b**, **c**), 10 μm (**d**–**f**)

(1:100 dilution, Chemicon International, Calif.). Rhodamine-conjugated pig anti-rabbit IgG (DakoCytomation, Glostrup, Denmark) and pig anti-sheep IgG (Eappel, Biochemical Division, Auroa, Ohio), both diluted 1:200, were then applied for 60 min at room temperature. The stained cells were mounted and sealed with a PBS-glycerol mixture (1:9 v/v) containing DAPI (4,6-diamidino-2-phenylindole) diluted 1:2,000. Non-immune sera of sheep and rabbit were used instead of primary antibodies as a control.

RNA preparation

Total RNA was isolated, by using TRIZOL REAGENT (Invitrogen Life Technologies) according to the manufac-

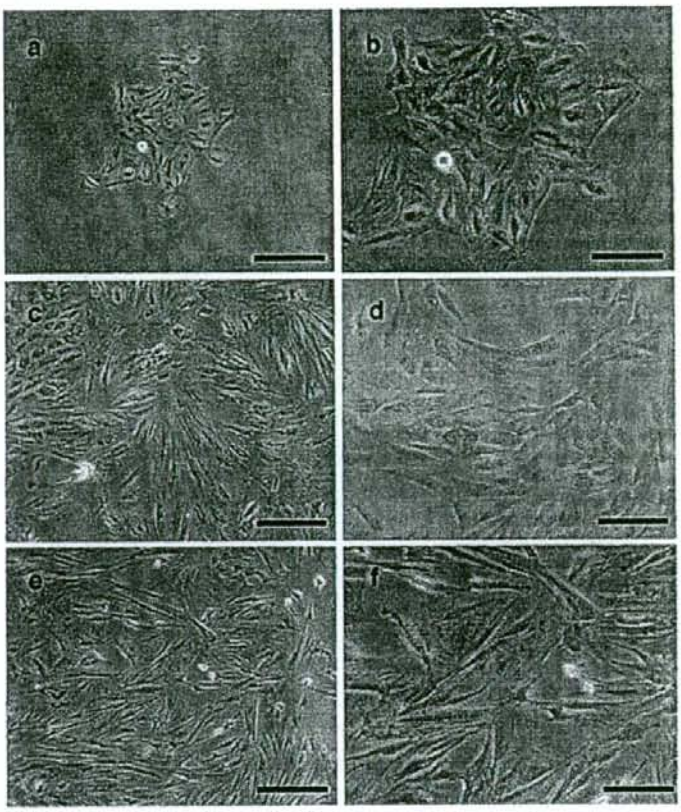

Fig. 2 Cell morphology by phase-contrast microscopy. **a** At culture day 14, DFC-I formed small colonies. **b** Higher magnification of **a** showing the polygonal appearance of the cells at passage 1. **c** At culture day 7, periodontal ligament cells (PDLC) at passage 3 showed a fibroblastic morphology. **d** Higher magnification of **c** showing either spindle- or polygonal-shaped PDLC. **e** At culture day 7, bone marrow stromal cells (BMSC) at passage 3 were more fibroblastic in morphology than the PDLC. **f** At higher magnification, BMSC were either spindle or polygonal in shape. *Bars* 100 μm (**a**, **c**, **e**), 50 μm (**b**, **d**, **f**)

turer's instructions, from the DF at the early crown-formation stage, DFC at the 10th passage, DFC-I at the 10th passage cultured on P-d and Col-I-d, PDLC, BMSC, and implants at 1, 2, and 4 weeks after transplantation.

RNA analyses

cDNA were synthesized from 1 μg total RNA in a 20-μl reaction containing 10× reaction buffer, 5 mM dNTP mixture, 1 U/μl RNase inhibitor, 0.25 U/μl reverse transcriptase (M-MLV reverse transcriptase, Invitrogen), and 0.125 μM random primers (Takara, Tokyo, Japan). For sq-PCR, amplification was performed in a PCR Thermal Cycler SP (Takara) for 25-35 cycles according to the following reaction profile: 95°C for 30 s, 45-60°C for 30 s, and 72°C for 30 s. Porcine glyceraldehyde-3-phosphate dehydrogenase (GAPDH) primers were used as internal standards. The percentage of mRNA expression in the implants from the in vivo gene expression analysis was measured by using Scion Image picture-imaging software (Scion, Frederick, Md.). Synthesized cDNA served as a template for subsequent PCR amplification with specific primers as listed in Table 1.

Real-time PCR was performed to quantify absolute mRNA expression by using the ABI PRISM 7900HT (Applied Biosystems, CA) with Absolute QPCR SYBR Green Mixes (Applied Biosystems). Primers were designed by using Primer-Express software (Applied Biosystems); the sequences are listed in Table 2. The thermocycling parameters were optimized at 50°C for 2 min, 95°C for 15 min, and 40 cycles of 95°C for 15 s and 61°C for 1 min. Cycle threshold (Ct) values were determined and employed to calculate relative gene amounts. The specificity of the PCR products was evaluated from the melt temperature (Tm) of the PCR products by using dissociation curve analysis. PCR products were quantified by means of Microsoft Excel (Microsoft, Wash.) to compare the amplification of the target genes with that of GAPDH as a reference gene, with calibrator normalization and amplification efficiency correction. All experiments were repeated three times, and significant statistical differences were determined by Student's *t*-test ($P<0.05$).

Table 1 Sequences of primer pairs used for reverse-transcription polymerase chain reaction (*CTGF* connective tissue growth factor, *GAPDH* glyceraldehyde-3-phosphate dehydrogenase)

Gene	Sequence	Annealing temperature (°C)	Products (bp)	Accession number or reference
Collagen type I	Forward 5′-GATCCTGCTGACGTGGCCAT Reverse 5′-ACTCGTGCAGCCGTCGTAGA	55	212	AY350905
Collagen type III	Forward 5′-TCCCCAGCAAAAGATTTCAC Reverse 5′-AGCACCATTGAGACATTTGAA	45	237	AJ289758
Bone sialoprotein	Forward 5′-ACTGAAGCCCAAGGAACCAC Reverse 5′-TCCAACGTGGTCTTCTGGAC	48	480	L10363
Runx2/cbfa1	Forward 5′-GACCCTGGAAGGAAACACAA Reverse 5′-CGCTGGTCCATGCTTAGAGT	56	303	Iohara et al. 2004
Osteocalcin	Forward 5′-TCAACCCCGACGACGAG Reverse 5′-GACCGTCGACRAAACCCTGA	60	204	AY150038
Osteopontin	Forward 5′-GCAATGAGCATTCCAATGTG Reverse 5′-GACCGTCGACTAAACCCTGA	56	383	X16575
Periostin	Forward 5′-CTGCACATGCAAGGATGACT Reverse 5′-ACATGGAGTTTCCCAGGCTA	54	589	AY880669
Biglycan	Forward 5′-GATGGCCTGAAGCTCAA Reverse 5′-GGTTGTTGAAGAGGCTG	60	406	AF159382
CTGF	Forward 5′-GCTCTTCTTCATGACCTCACCGT Reverse 5′-GCGGCTTACCGACTGGAAGACAC	60	411	U70060
GAPDH	Forward 5′-TCGACCACAGGGTAGGTTTC Reverse 5′-CCCCAGCATCAAAGGTAGAA	45	497	AF017079

Measurement of cell proliferation

DFC-I were plated at a density of 5×10^3 cells/ml into 6-well Col-I-d and standard tissue-grade P-d (BD Biosciences, Mountain View, Calif.). The DFC-I in each well were counted by using a WST-8 kit (Cell-counting Kit-8; Dojindo Laboratories, Kumamoto, Japan). The counting technique employed a tetrazolium salt that produces a highly water-soluble formazan dye. After a 1-h incubation with reagent according to the manufacturer's instructions, the relative cell number was determined by measuring the absorbance of light at a wavelength of 450 nm at days 1, 7, and 14 (Model 650 Microplate Reader; Biorad Laboratories, Hercules, Calif.).

Assay for ALPase activity

DFC-I were plated at density of 5×10^3 cells/ml into 6-well Col-I-d and P-d (BD Biosciences). For quantitative analysis of ALPase activity, *p*-nitrophenol production was measured at 37°C for 6 min in Milli-Q water by using a Fast *p*-

Table 2 Sequence of primer pairs for real-time polymerase chain reaction (*GAPDH* glyceraldehyde-3-phosphate dehydrogenase)

Gene	Sequence	Annealing temperature (°C)	Products (bp)	Accession number
Collagen type I	Forward 5′-TCAAAGTCTTCTGCAACATGGAG Reverse 5′-GGCACGCTGGGCTGAG	61	79	AY350905
Collagen type III	Forward 5′-TTGGCCCTGTTTGCTTTTTATAA Reverse 5′-CAAAAGGAACACATATGGAGTGTGA	61	82	AJ289758
Bone sialoprotein	Forward 5′-CCGAGGCCGAGAATATCACTC Reverse 5′-TTCCCGGCGTTACGTCC	61	66	L10363
Osteocalcin	Forward 5′-CTGGCTGATCACATCGGCT Reverse 5′-GCGAGGTCTAGGCTATGCCAT	61	64	AY150038
Osteopontin	Forward 5′-GCTGTCCCCACGGGAGA Reverse 5′-TTTTGACCTCAGTCCATAGACCAC	61	66	X166575
Periostin	Forward 5′-GGTCACAGACGTGGATTGGAT Reverse 5′-CCAGTTGGAGCTGTAGCCACT	61	71	AY880669
Biglycan	Forward 5′-AACGGGAGCCTGAGTTTTCTG Reverse 5′-CACCCTGGACAGCTTGTTGTT	61	69	AF159382
GAPDH	Forward 5′-GGGTCATCATCTCTGCCCCT Reverse 5′-CTCATGGTTCACGCCCACT	61	68	AF017079

nitrophenyl phosphate tablet set (Sigma) as a substrate. The relative amount of *p*-nitrophenol was estimated from the light absorbance at a wavelength of 405 nm at days 1, 7, and 14 (Bio-Rad Laboratories).

In vivo differentiation assay

The differentiation potential of individual DFC-I on transplantation into immunodeficient mice was assessed as described previously (Handa et al. 2002). Briefly, 1.5×10^6 DFC-I were incubated in a mixture of 40 mg β-tricalcium phosphate powder (TCP; Osferion G1, no. BH064005, Olympus Biomaterials, Tokyo, Japan) and fibrin clot (mixture of mouse fibrinogen and thrombin; both from Sigma) and were then inoculated subcutaneously into 5-week-old female CB-17 scid/scid (scid; severe combined immunodeficiency) mice (Nihoncrea, Tokyo, Japan). Mice were sacrificed after 1, 2, 4, and 8 weeks. The implants removed at 1, 2, and 4 weeks after transplantation were cut in half for histochemical analysis, calcification analysis, and mRNA expression analysis of periodontium matrix components. The implants removed at 8 weeks after transplantation were only used for histological analysis.

At 4 and 8 weeks after transplantation, the implants were fixed, decalcified with 10% EDTA-2Na, and then processed for histological examination by using standard procedures. Sections were stained with hematoxylin-eosin for histological observation and prepared for immunohistochemistry.

Immunohistochemical analysis was performed by using the Vectastain ABC kit (Vector Laboratories), as previously described (Hsu et al. 1981) with modification (Chen et al. 1991a). The antibody used was an affinity-purified rabbit anti-pig BSP polyclonal antibody (gift from Dr. J. Sodek, University of Toronto, Canada) (1:2,000 dilution). To determine the potential for hard tissue formation in the DFC-I, we selected 15 sections at random from at least five specimens.

The Von Kossa staining procedure was also performed to analyze the extent of calcification in hard tissue, as described previously (Piattelli et al. 1994).

Results

Porcine third molar at early crown-formation stage

The 6-month porcine third molar appeared at the crown-formation stage (Fig. 1a), with the formation of hard tissues being well advanced. The DF was clearly distinguished from the dental enamel organ and enamel at high magnifi-

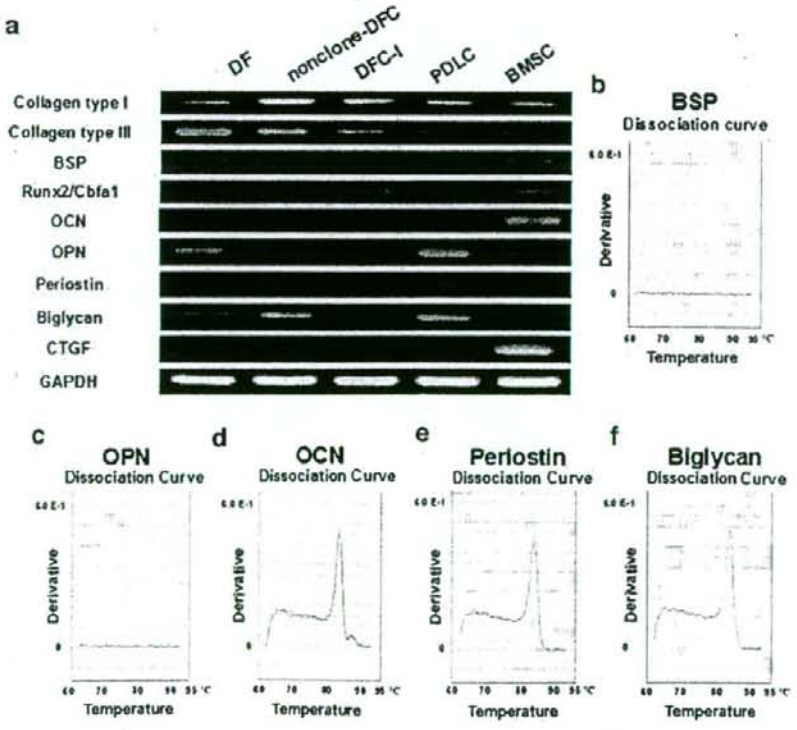

Fig. 3 **a** Semiquantitative RT-PCR analysis of osteoblast-lineage/periodontal ligament-related genes in DF, nonclone-DFC, DFC-I, PDLC, and BMSC. In DFC-I, there was no detectable expression of mature cementoblast/osteoblast markers such as bone sialoprotein (*BSP*), osteopontin (*OPN*), osteocalcin (*OCN*), connective tissue growth factor (*CTGF*), and biglycan, and no periostin. The expression of OPN, biglycan, and BMP-4 was higher in PDLC than in BMSC, but Runx2/Cbfa1, CTGF, and ALPase showed lower expression in PDLC than in BMSC. **b–f** Melting profile of the amplicon of BSP, OPN, OCN, periostin, and biglycan in DFC-I by real-time RT-PCR. Results were obtained by using the Sequence Detection Systems of dissociation curve software. OCN, periostin, and biglycan expressions were detected in DFC-I, but BSP and OPN were not detected

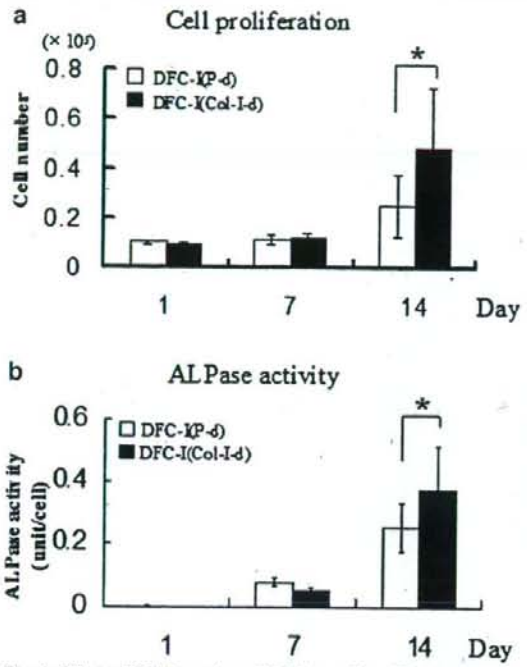

Fig. 4 Effects of Col-I matrix on DFC-I on cell proliferation (**a**) and ALPase activity (**b**). The cells were seeded at a density of 5.0×10^3 cells in standard 6-well plates (*P-d*) or in 6-well plates coated by Col-I (*Col-I-d*). No significant differences were apparent at 1 and 7 days. At 14 days, cell proliferation and ALPase activity of DFC-I cultured on Col-I-d were significantly higher than those on P-d. *Statistically significant at $P<0.05$ (paired *t*-test)

cation by the increased collagen fibrils occupying the extracellular spaces between the follicular fibroblasts (Fig. 1b). ECM in the DF was positive for the Col-I mesenchymal marker by immunohistochemistry (Fig. 1c).

Immunofluorescent staining of DFC

Immunofluorescent staining was then carried out to determine the lineage of the isolated cells by using antibodies specific for vimentin (Fig. 1d) and Col-I (Fig. 1e) as mesenchymal markers, and an anti-cytokeratin14 antibody as an epithelial marker (Fig. 1f). All isolated cells were positive for Col-I and vimentin and negative for cytokeratin14 (nuclei showed blue DAPI staining). These results demonstrated that all isolated cells were derived from mesenchyme with no contamination from dental epithelial cells.

Purification of DFC

One DFC-I colony was expanded and analyzed over a number of weeks in culture, producing a cumulative expansion in the single cell clones for over 30 passages prior to the onset of cellular senescence. Overall, six clones were expanded; the other clones exhibited only moderate growth potential that did not persist beyond 20 passages. The DFC-I comprised polygonal cells (Fig. 2a,b), whereas both the PDLC (Fig. 2c,d) and BMSC (Fig. 2e,f) had a mixed morphology including spindle-shaped and polygonal-shaped cells.

Gene expression pattern of DFC-I

We surveyed gene expression patterns in the DF, nonclone-DFC, DFC-I, PDLC, and BMSC by sq-PCR analysis (Fig. 3a). A series of genes are known to be involved in the morphogenesis of periodontium and bone (Table 1). The expression patterns of three DF-related genes in the DF, nonclone-DFC, and DFC-I were markedly different. mRNA expression for BSP and osteopontin (OPN) was only detected in the DF. Biglycan was expressed only in the DF and nonclone-DFC. From these results, the expression pattern of DFC-I resembled the more immature stage. Differences were also found when we compared the gene expression profiles of DFC-I, PDLC, and BMSC. BSP, OCN, and connective tissue growth factor (CTGF) expression was detected only in BMSC, whereas OPN, periostin, and biglycan were expressed only in the PDLC and BMSC. Runx2/Cbfa1 mRNA was expressed in all cell types. The expression levels of GAPDH were consistent across samples. BSP, OCN, OPN, periostin, and biglycan were not detected in DFC-1 by sq-PCR, prompting further investigation by rt-PCR for these genes (Table 2). Surprisingly, cementoblast/osteoblast markers such as BSP and OPN were not detected in DFC-I, but periostin, biglycan,

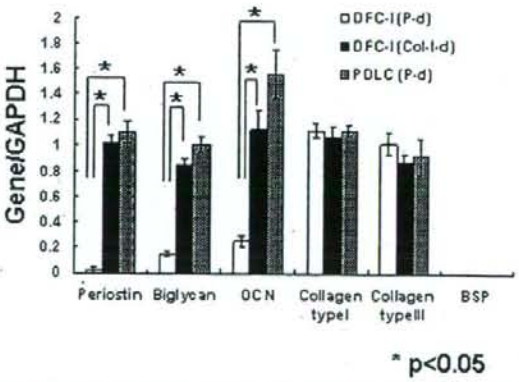

Fig. 5 Effects of Col-I matrix on mRNA expressions in DFC-I cultured on P-d and Col-d and in PDLC on P-d as measured by using real-time RT-PCR. DFC-I cultured on Col-I-d showed upregulated gene expression of periostin, biglycan, and OCN, whereas BSP were not expressed in any of the three cell classes. The results were consistent within three independent experiments. *Statistically significant at $P<0.05$ (paired *t*-test)

and OCN were expressed, albeit at a lower level in DFC-I than in PDLC and BMSC (Fig. 3b–f). These data suggested that DFC-I represented more immature cells compared with PDLC and BMSC.

Effect of Col-I matrix on cell proliferation and ALPase activity

After 1 and 7 days in culture, the cell proliferation of DFC-I cultured on Col-I-d was similar to that on P-d. After 14 days, DFC-I cultured on Col-I-d showed a significantly higher rate of cell proliferation compared with clones cultured on P-d (Fig. 4a). ALPase activity is a recognized mineralization marker in tissue (Alliot-Licht et al. 2005; Pavasant et al. 2003). The DFC-I cultured for 1, 7, and 14 days exhibited different and increasing levels of ALPase activity (Fig. 4b). At days 1 and 7 of culture, the ALPase activity change was the same regardless of culturing conditions, but at 14 days, DFC-I cultured on Col-I-d showed higher activity than those cultured on P-d (Fig. 4b). This

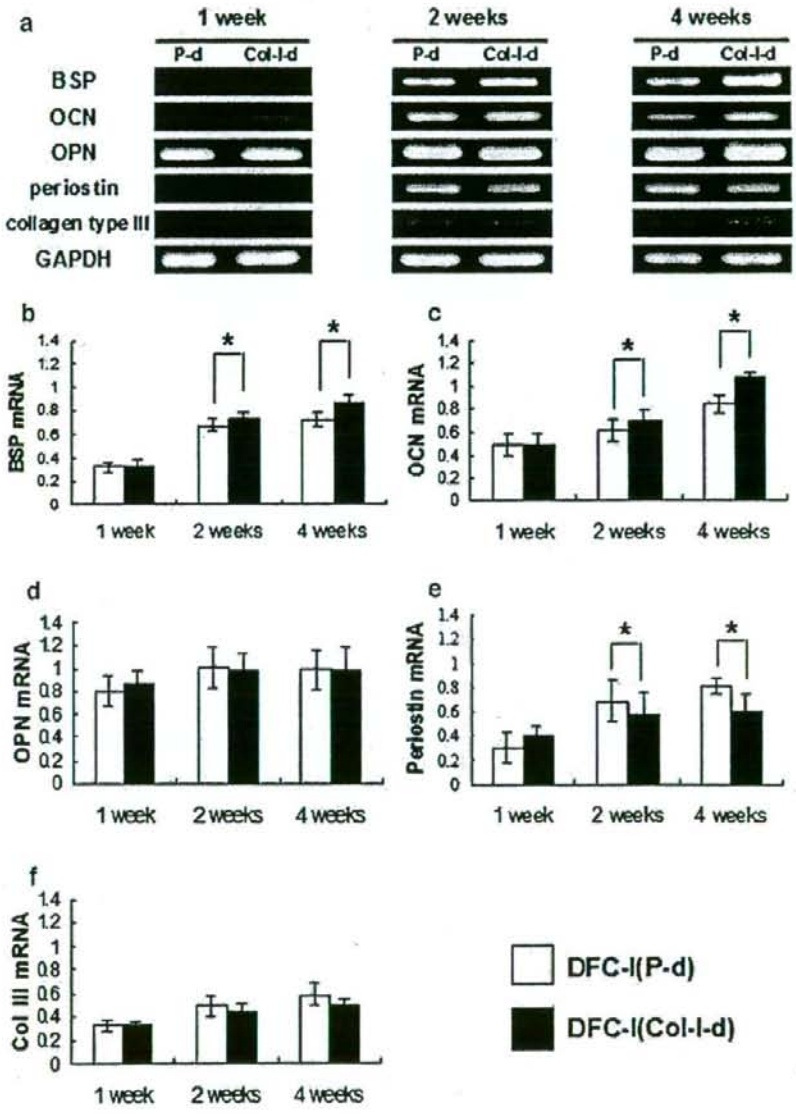

Fig. 6 Effects of Col-I matrix on gene expressions in DFC-I in vivo. **a** At 1 week, the BSP, periostin, and collagen type III genes were not expressed in either implant type but were clearly expressed at 2 and 4 weeks after transplantation. OCN and OPN genes were expressed strongly in both implant types at all time points. **b–f** Quantification of expression of BSP, OCN, OPN, periostin, and collagen type III genes by using Scion picture-imaging software. BSP and OCN genes were more highly expressed in the implants cultured on Col-I-d than in those on P-d at 2 and 4 weeks. In contrast, periostin expression was higher in implants on P-d at 2 and 4 weeks than in those cultured on Col-I-d. No significant difference in the expressions of OPN and collagen type III was seen for both implant types at all time points. *Statistically significant at $P<0.05$ (paired t-test)

result suggested that adhesion to Col-I promoted differentiation of the DFC-I.

Effect of Col-I on gene expressions in clone-DFC-I

We next investigated, by rt-PCR, the effect of Col-I culturing on gene expression in the DFC-I cells (Fig. 5). Putative markers of PDLC and cementoblasts/osteoblasts, such as periostin, biglycan, and OCN, were amplified more readily from DFC-I cultured on Col-I compared with DFC-I cultured on P-d. Periostin, biglycan, and OCN expression levels in DFC-I cultured on Col-I-d were approximately 100-fold, 6-fold, and 5-fold higher, respectively, than in DFC-I cultured on P-d. The expression levels of upregulated genes resembled levels of the same genes in PDLC, whereas the expression levels of Col-I and collagen type III showed no change, even in DFC-I cultured on Col-I. BSP was not expressed in DFC-I cultured on P-d or Col-I-d, or

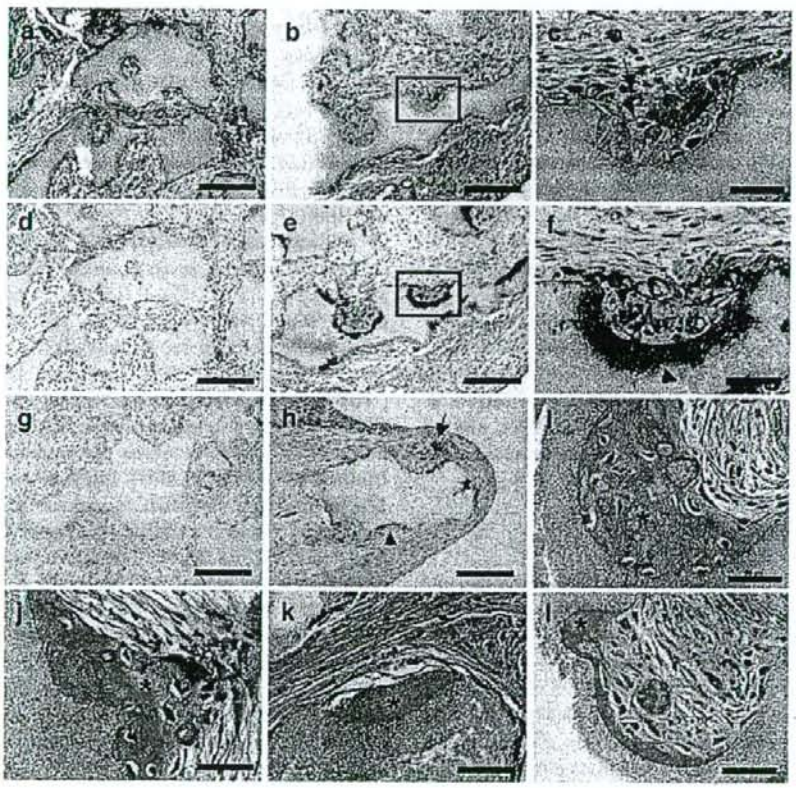

Fig. 7 **a–h** Morphology of representative implants of DFC-I cultured on P-d (**a**, **d**, **g**) or Col-I-d (**b**, **c**, **e**, **f**, **h**), at 4 weeks after transplantation. **a** No hard tissue formation was seen in the implants from P-d. Connective tissues were formed between the TCP particles. **b** A small amount of the hard tissue was produced in the implants from DFC-I cultured on Col-I-d. **c** Higher magnification of the *boxed area* in **b** showing the mineralized tissues on the surface of the TCP particles in the part of the implants cultured on Col-I-d. **d** No specific staining with the BSP antibody was observed in implants of DFC-I cultured on P-d. **e** Specific staining with BSP was clearly observed in the extracellular matrix of the cells lining the TCP particles from DFC-I cultured on Col-I-d. **f** Higher magnification of the *boxed area* in **e** showing specific staining for BSP in the cytoplasm of cells cultured on Col-I-d and on the surface of the TCP particles (*arrowheads*). **g** Implants of DFC-I cultured on P-d showed no positive Von Kossa staining. **h** Von Kossa staining showed clear mineral nodules (*arrow*) in the parts of implants of DFC-I cultured on Col-I-d and on the surface of the TCP particles (*arrowhead*). **i–l** Morphology of representative implants of DFC-I cultured on P-d (**i**, **k**) and Col-I-d (**j**, **l**), at 8 weeks after transplantation. **i** Hard tissue formation was clearly identified. Bone-like tissues were formed, and osteocyte-like cells were embedded in the part of implants of DFC-I cultured on P-d (*asterisk*). **j** The bone-like tissues were clearly visible in the implants from Col-I-d (*asterisk*). **k** Cementum-like tissues were formed and lined the TCP-particle surfaces (*asterisk*) in the part of implants cultured on P-d. **l** Cementum-like tissues were formed and lined the TCP-particle surfaces in the part of the implants from Col-I-d culture (*asterisk*). No clear differences were apparent in the amount of hard tissue formation in the implants from DFC-I cultured on Col-I-d compared with P-d. *Bars* 200 μm (**a**, **b**, **d**, **e**, **g**, **h**), 100 μm (**c**, **f**, **i**, **j**, **k**, **l**)

in PDLC. These results demonstrated that gene expression patterns in DFC-I cultured on Col-I resembled those of PDLC.

Developmental potential of clone-DFC-I in vivo

In vivo characterization of clone-DFC-I

To extend the comparison of DFC-I cultured on Col-I-d and on P-d, we investigated the potential for mineralization in vivo by transplanting DFC-I in conjunction with TCP into the subcutaneous tissue of immunocompromised scid mice as described previously (Handa et al. 2002; Saito et al. 2005). At 1, 2, and 4 weeks after transplantation, we examined the relevant gene expression in the implants by sq-PCR. No expression of the BSP or periostin genes was seen at 1 week after transplantation in either implant type (DFC-I cultured on Col-I-d versus P-d), but clear expression was detected at 2 and 4 weeks (Fig. 6a,b). Periostin expression was distinctly lower in Col-I-d-cultured implants than in P-d-cultured implants (Fig. 6a,e). OCN and OPN expression was strongly detected in both implants at 4 weeks, with higher levels being detected in the Col-I-d-cultured implants than in those cultured on P-d (Fig. 6a,c,d). Collagen type III expression in implants from both dish types was just detectable at 1 week and gradually increased at 2 and 4 weeks, with no differences in expression levels between culturing conditions (Fig. 6a,f).

In vivo histochemical analysis

At 4 weeks, no hard tissue was apparent in control implants (Fig. 7a), but a small amount of calcified tissue was observed in the experimental group (Fig. 7b,c). We therefore performed immunohistochemical staining on the complex of TCP and developing DFC to examine this possibility in more detail. Some of the cells lining the TCP particles were positive for BSP antibody staining in the experimental group (Fig. 7e,f), whereas no positive staining was detected in the control group (Fig. 7d). Furthermore, Von Kossa staining was performed to investigate whether DFC-I cells cultivated on Col-I-d would promote the formation of mineralized nodules. This staining revealed substantial mineralization of tissue in the implants with DFC-I cultivated on Col-I-d (Fig. 7h), but not in the implants with DFC-I cultivated on P-d (Fig. 7g). These results indicated that DFC-I under Col-I culture conditions had an advanced ability to induce hard tissue formation.

At 8 weeks, hard tissues were identified in both implants on the surface of TCP particles and in the cells (Fig. 7i–l), with no obvious difference between the two experimental groups.

Discussion

We have obtained one clonal cell population (DFC-I) from porcine cultured DFC isolated from developing teeth at the early crown-formation stage. Although previous studies have analyzed DFC from the root surface during root formation, no data exist for cells at the early crown-formation stage (Hakki et al. 2001; Handa et al. 2002; Jin et al. 2003; Saito et al. 2005). The isolation of progenitor cells from the DF may therefore help to identify the as-yet-unknown mechanism for differentiation into the cementoblasts, PDL fibroblasts, and osteoblasts that make up the periodontium (Lekic et al. 1996; Pitaru et al. 1994). The properties exhibited by a single cell clone population could possibly be used to elucidate the mechanisms of differentiation. Based on these ideas, we have propagated and characterized DFC-I with respect to the expression of several marker genes preferentially expressed in PDLC and BMSC (Table 1).

Characterization of the DFC-I gene expression pattern has revealed inconsistencies from the patterns among DF, nonclone-DFC, PDLC, and BMSC. Comparison of our DFC-I with PDLC and BMSC has shown that most osteogenesis-related genes including BSP, OPN, and CTGF are not detectable in DFC-I, although BSP, OPN, and CTGF have been detected in DF and BMSC. Normally, OPN is expressed followed first by BSP and subsequently by OCN, which characterizes the postproliferative phase (Aubin 2001; Liu et al. 2003). Biglycan is a small leucine-rich proteoglycan that binds to various ECM components and has a role in mineralization (Xu et al. 1998). With regard to PDLC, no clear differentiation marker specifically characterizes this type of cell, especially in the pig. In this study, periostin expression has been weakly detected in DFC-I, but strongly in PDLC. Taken together, our results demonstrate the low expression of genes related to osteogenesis in the DFC-I, despite the ECM being osteogenic at this stage of development. Although the DF consists of heterogeneous cell populations, our findings suggest that DFC-I is an immature cell type, distinct from both PDLC and BMSC. Recently, three types of DFC have been reported (Luan et al. 2006). Further examination of the other clone-cell populations obtained in the present study from one tooth bud at the early crown-formation stage is therefore required.

As a second aim of this study, we have evaluated the effect of a Col-I matrix on DFC-I. Col-I is well known to interact with $\alpha 1\beta 1$, $\alpha 2\beta 1$, and $\alpha 3\beta 1$ integrin receptors via the DGEA amino acid sequence (Staatz et al. 1991). A previous study has demonstrated that Col-I regulates OCN gene expression, and the mRNA level of OCN gene expression is upregulated in dental pulp cells (Mizuno et al. 2003). By immunohistochemistry, we have shown that

Col-I is a major component of the DF. We have further shown that ALPase activity is higher in Col-I-treated DFC-I, suggesting a role for Col-I in stimulating the differentiation of DFC-I. Sasaki et al. (1990) have shown intense ALPase activity along the plasma membranes of whole cell surfaces in cementoblasts of human deciduous teeth. Moreover, PDLC also express high ALPase activity (Giannopoulou and Cimasoni 1996; Ogata et al. 1995) in vitro in the presence of osteogenic medium (Nohutcu et al. 1997; Ramakrishnan et al. 1995). These findings are in agreement with our results.

We have further explored the expression of genes associated with the periodontium. DFC are similar to odontoblasts and osteoblasts in terms of mineralized tissue formation (Gronthos et al. 2000; Shi et al. 2001). However, the gene expression of BSP has not been found to be upregulated by Col-I in our study. Our results are therefore not consistent with expression patterns in dental pulp and MSCs. On the other hand, Col-I potently stimulates the expression of periostin, biglycan, and OCN in DFC-I. A recent study has shown that PDLC lines and osteoblasts share the expression of gene for periostin but not the genes for BSP or OCN (Saito et al. 2002). Biglycan facilitates the initiation of apatite formation and inhibits the growth of apatite in a gelatin gel system (Boskey et al. 1997). Our results are consistent with these observations and suggest that the expression pattern of DFC-I exposed to Col-I resembles those of PDLC. Together, the results of the ALPase activity and gene expression analyses therefore indicate that a Col-I matrix influences the differentiation of immature DFC along the osteogenic pathway, as for PDLC. However, the limited data obtained from one specific cell population in the present study may be insufficient to provide information on this issue. Therefore, further study is needed on the other clone populations.

Finally, we tested whether DFC-I have the capacity to produce hard tissue. Progenitor cells isolated from bovine DF at the root-formation stage have previously been shown to generate cementum (Handa et al. 2002); however, no data exist for DFC at the early crown-formation stage. Examination of the gene expression patterns related to osteogenesis has revealed the expression of BSP at 2 weeks after transplantation, and OCN, periostin, and collagen type III expressions gradually increase. OCN appears immediately before the start of mineralization (Nakashima 1994), and BSP mRNA is expressed almost exclusively in differentiated osteoblasts, odontoblasts, and cementoblasts (Bianco et al. 1991; Chen et al. 1991b, 1992). Significant differences occur in BSP and periostin expression at 2 and 4 weeks and in OCN at 4 weeks between implants cultured on Col-I-d versus P-d and suggest that Col-I promotes follicle cells in the TCP particles to differentiate along a mineralization pathway in vivo.

The implants in control groups at 4 weeks have no hard tissues, whereas the implants of the experiment group show a small extent of calcification by Von Kossa staining. In addition, a significant difference has been observed in BSP immunostaining. When DFC cultured on Col-I are implanted, the cells lining the TCP particles are BSP-immunostained, but this is not seen with P-d. At 8 weeks, hard tissue formation is apparent in both groups. These findings therefore suggest that the DFC-I under the TCP particles develop into a cementoblast/osteoblast lineage capable of forming a mineralized ECM, and that Col-I facilitates this differentiation in vivo. However, specific factors promoting this differentiation have not been identified in these studies.

Up to now, PDLC have been obtained from the tooth-root surface to establish periodontal-tissue engineering (Akizuki et al. 2005; Hasegawa et al. 2005). Thus, a tooth has to be extracted to obtain periodontal tissues. Most people have an impacted third molar that does not cause occlusion. The DF usually involves impacted third molars, which are often extracted for orthodontic therapy. The use of impacted third molars as a cell source for periodontal-tissue engineering might expand the avenues for treatment of disease in this field. The present DF study may be a promising first step toward complete periodontal-tissue engineering.

Acknowledgments We thank Dr. J. Sodek for generously providing the collagen type I and BSP antibodies (University of Toronto, Canada), Dr. H. Irie for the kind gift of the Osferion G1 (Olympus, Japan), and Dr. A. Kamiya (IMSUT, Japan) for technical support.

References

Akintoye SO, Lam T, Shi S, Brahim J, Collins MT, Robey PG (2006) Skeletal site-specific characterization of orofacial and iliac crest human bone marrow stromal cells in same individuals. Bone 38:758–768

Akizuki T, Oda S, Komaki M, Tsuchioka H, Kawakatsu N, Kikuchi A, Yamato M, Okano T, Ishikawa I (2005) Application of periodontal ligament cell sheet for periodontal regeneration: a pilot study in beagle dogs. J Periodontal Res 40:245–251

Alliot-Licht B, Bluteau G, Magne D, Lopez-Cazaux S, Lieubeau B, Daculsi G, Guicheux J (2005) Dexamethasone stimulates differentiation of odontoblast-like cells in human dental pulp cultures. Cell Tissue Res 321:391–400

Aubin JE (2001) Regulation of osteoblast formation and function. Rev Endocr Metab Disord 2:81–94

Bartold PM, Miki Y, McAllister B, Narayanan AS, Page RC (1988) Glycosaminoglycans of human cementum. J Periodontal Res 23:13–17

Bianco P, Fisher LW, Young MF, Termine JD, Robey PG (1991) Expression of bone sialoprotein (BSP) in developing human tissues. Calcif Tissue Int 49:421–426

Bianco P, Riminucci M, Gronthos S, Robey PG (2001) Bone marrow stromal stem cells: nature, biology, and potential applications. Stem Cells 19:180–192

Boskey AL, Spevak L, Doty SB, Rosenberg L (1997) Effects of bone CS-proteoglycans, DS-decorin, and DS-biglycan on hydroxyapatite formation in a gelatin gel. Calcif Tissue Int 61:298–305

Chen J, Zhang Q, McCulloch CA, Sodek J (1991a) Immunohistochemical localization of bone sialoprotein in foetal porcine bone tissues: comparisons with secreted phosphoprotein 1 (SPP-1, osteopontin) and SPARC (osteonectin). Histochem J 23:281–289

Chen JK, Shapiro HS, Wrana JL, Reimers S, Heersche JN, Sodek J (1991b) Localization of bone sialoprotein (BSP) expression to sites of mineralized tissue formation in fetal rat tissues by in situ hybridization. Matrix 11:133–143

Chen J, Shapiro HS, Sodek J (1992) Development expression of bone sialoprotein mRNA in rat mineralized connective tissues. J Bone Miner Res 7:987–997

Diekwisch TG (2001) The developmental biology of cementum. Int J Dev Biol 45:695–706

Ducy P, Starbuck M, Priemel M, Shen J, Pinero G, Geoffroy V, Amling M, Karsenty G (1999) A Cbfa1-dependent genetic pathway controls bone formation beyond embryonic development. Genes Dev 13:1025–1036

Giannopoulou C, Cimasoni G (1996) Functional characteristics of gingival and periodontal ligament fibroblasts. J Dent Res 75:895–902

Gronthos S, Mankani M, Brahim J, Robey PG, Shi S (2000) Postnatal human dental pulp stem cells (DPSCs) in vitro and in vivo. Proc Natl Acad Sci USA 97:13625–13630

Hakki SS, Berry JE, Somerman MJ (2001) The effect of enamel matrix protein derivative on follicle cells in vitro. J Periodontol 72:679–687

Han X, Amar S (2003) IGF-1 signaling enhances cell survival in periodontal ligament fibroblasts vs. gingival fibroblasts. J Dent Res 82:454–459

Handa K, Saito M, Tsunoda A, Yamauchi M, Hattori S, Sato S, Toyoda M, Teranaka T, Narayanan AS (2002) Progenitor cells from dental follicle are able to form cementum matrix in vivo. Connect Tissue Res 43:406–408

Hasegawa M, Yamato M, Kikuchi A, Okano T, Ishikawa I (2005) Human periodontal ligament cell sheets can regenerate periodontal ligament tissue in an athymic rat model. Tissue Eng 11:469–478

Hsu SM, Raine L, Fanger H (1981) Use of avidin-biotin-peroxidase complex (ABC) in immunoperoxidase techniques: a comparison between ABC and unlabeled antibody (PAP) procedures. J Histochem Cytochem 29:577–580

Iohara K, Nakashima M, Ito M, Ishikawa M, Nakasima A, Akamine A (2004) Dentin regeneration by dental pulp stem cell therapy with recombinant human bone morphogenetic protein 2. J Dent Res 83:590-595

Jin QM, Zhao M, Webb SA, Berry JE, Somerman MJ, Giannobile WV (2003) Cementum engineering with three-dimensional polymer scaffolds. J Biomed Mater Res [A] 67:54–60

Klees RF, Salasznyk RM, Kingsley K, Williams WA, Boskey A, Plopper GE (2005) Laminin-5 induces osteogenic gene expression in human mesenchymal stem cells through an ERK-dependent pathway. Mol Biol Cell 16:881–890

Lekic P, Sodek J, McCulloch CA (1996) Relationship of cellular proliferation to expression of osteopontin and bone sialoprotein in regenerating rat periodontium. Cell Tissue Res 285:491–500

Lekic P, Rojas J, Birek C, Tenenbaum H, McCulloch CA (2001) Phenotypic comparison of periodontal ligament cells in vivo and in vitro. J Periodontal Res 36:71–79

Liu F, Malaval L, Aubin JE (2003) Global amplification polymerase chain reaction reveals novel transitional stages during osteoprogenitor differentiation. J Cell Sci 116:1787–1796

Luan X, Ito Y, Dangaria S, Diekwisch TG (2006) Dental follicle progenitor cell heterogeneity in the developing mouse periodontium. Stem Cells Dev 15:595–608

Marcopoulou CE, Vavouraki HN, Dereka XE, Vrotsos IA (2003) Proliferative effect of growth factors TGF-beta1, PDGF-BB and rhBMP-2 on human gingival fibroblasts and periodontal ligament cells. J Int Acad Periodontol 5:63–70

Mizuno M, Kuboki Y (2001) Osteoblast-related gene expression of bone marrow cells during the osteoblastic differentiation induced by type I collagen. J Biochem (Tokyo) 129:133–138

Mizuno M, Miyamoto T, Wada K, Watatani S, Zhang GX (2003) Type I collagen regulated dentin matrix protein-1 (Dmp-1) and osteocalcin (OCN) gene expression of rat dental pulp cells. J Cell Biochem 88:1112–1119

Morsczeck C, Gotz W, Schierholz J, Zeilhofer F, Kuhn U, Mohl C, Sippel C, Hoffmann KH (2005) Isolation of precursor cells (PCs) from human dental follicle of wisdom teeth. Matrix Biol 24:155–165

Murakami Y, Kojima T, Nagasawa T, Kobayashi H, Ishikawa I (2003) Novel isolation of alkaline phosphatase-positive subpopulation from periodontal ligament fibroblasts. J Periodontol 74:780–786

Nakao K, Itoh M, Tomita Y, Tomooka Y, Tsuji T (2004) FGF-2 potently induces both proliferation and DSP expression in collagen type I gel cultures of adult incisor immature pulp cells. Biochem Biophys Res Commun 325:1052–1059

Nakashima M (1994) Induction of dentin formation on canine amputated pulp by recombinant human bone morphogenetic proteins (BMP)-2 and -4. J Dent Res 73:1515–1522

Nohutcu RM, McCauley LK, Koh AJ, Somerman MJ (1997) Expression of extracellular matrix proteins in human periodontal ligament cells during mineralization in vitro. J Periodontol 68: 320–327

Ogata Y, Niisato N, Sakurai T, Furuyama S, Sugiya H (1995) Comparison of the characteristics of human gingival fibroblasts and periodontal ligament cells. J Periodontol 66:1025–1031

Ouyang H, McCauley LK, Berry JE, D'Errico JA, Strayhorn CL, Somerman MJ (2000) Response of immortalized murine cementoblasts/periodontal ligament cells to parathyroid hormone and parathyroid hormone-related protein in vitro. Arch Oral Biol 45: 293–303

Palmer RM, Lumsden AG (1987) Development of periodontal ligament and alveolar bone in homografted recombinations of enamel organs and papillary, pulpal and follicular mesenchyme in the mouse. Arch Oral Biol 32:281–289

Pavasant P, Yongchaitrakul T, Pattamapun K, Arksornnukit M (2003) The synergistic effect of TGF-beta and 1,25-dihydroxyvitamin D3 on SPARC synthesis and alkaline phosphatase activity in human pulp fibroblasts. Arch Oral Biol 48:717–722

Piattelli A, Trisi P, Passi P, Piattelli M, Cordioli GP (1994) Histochemical and confocal laser scanning microscopy study of the bone-titanium interface: an experimental study in rabbits. Biomaterials 15:194–200

Pitaru S, McCulloch CA, Narayanan SA (1994) Cellular origins and differentiation control mechanisms during periodontal development and wound healing. J Periodontal Res 29:81–94

Pitaru S, Pritzki A, Bar-Kana I, Grosskopf A, Savion N, Narayanan AS (2002) Bone morphogenetic protein 2 induces the expression of cementum attachment protein in human periodontal ligament clones. Connect Tissue Res 43:257–264

Ramakrishnan PR, Lin WL, Sodek J, Cho MI (1995) Synthesis of noncollagenous extracellular matrix proteins during development of mineralized nodules by rat periodontal ligament cells in vitro. Calcif Tissue Int 57:52–59

Ruch JV (1998) Odontoblast commitment and differentiation. Biochem Cell Biol 76:923–938

Saito Y, Yoshizawa T, Takizawa F, Ikegame M, Ishibashi O, Okuda K, Hara K, Ishibashi K, Obinata M, Kawashima H (2002) A cell line with characteristics of the periodontal ligament fibroblasts is negatively regulated for mineralization and Runx2/Cbfa1/Osf2

activity, part of which can be overcome by bone morphogenetic protein-2. J Cell Sci 115:4191–4200

Saito M, Handa K, Kiyono T, Hattori S, Yokoi T, Tsubakimoto T, Harada H, Noguchi T, Toyoda M, Sato S, Teranaka T (2005) Immortalization of cementoblast progenitor cells with Bmi-1 and TERT. J Bone Miner Res 20:50–57

Salasznyk RM, Williams WA, Boskey A, Batorsky A, Plopper GE (2004) Adhesion to vitronectin and collagen I promotes osteogenic differentiation of human mesenchymal stem cells. J Biomed Biotechnol 2004:24–34

Sasaki T, Watanabe C, Shimizu T, Debari K, Segawa K (1990) Possible role of cementoblasts in the resorbant organ of human deciduous teeth during root resorption. J Periodontal Res 25:143–151

Saygin NE, Giannobile WV, Somerman MJ (2000) Molecular and cell biology of cementum. Periodontology 24:73–98

Shi S, Robey PG, Gronthos S (2001) Comparison of human dental pulp and bone marrow stromal stem cells by cDNA microarray analysis. Bone 29:532–539

Staatz WD, Fok KF, Zutter MM, Adams SP, Rodriguez BA, Santoro SA (1991) Identification of a tetrapeptide recognition sequence for the alpha 2 beta 1 integrin in collagen. J Biol Chem 266:7363–7367

Ten Cate AR, Mills C (1972) The development of the periodontium: the origin of alveolar bone. Anat Rec 173:69–77

Ten Cate AR, Mills C, Solomon G (1971) The development of the periodontium. A transplantation and autoradiographic study. Anat Rec 170:365–379

Thesleff I, Mikkola M (2002) The role of growth factors in tooth development. Int Rev Cytol 217:93–135

Wise GE, Lin F, Fan W (1992) Culture and characterization of dental follicle cells from rat molars. Cell Tissue Res 267:483–492

Xiao G, Wang D, Benson MD, Karsenty G, Franceschi RT (1998) Role of the alpha2-integrin in osteoblast-specific gene expression and activation of the Osf2 transcription factor. J Biol Chem 273: 32988–32994

Xu T, Bianco P, Fisher LW, Longenecker G, Smith E, Goldstein S, Bonadio J, Boskey A, Heegaard AM, Sommer B, Satomura K, Dominguez P, Zhao C, Kulkarni AB, Robey PG, Young MF (1998) Targeted disruption of the biglycan gene leads to an osteoporosis-like phenotype in mice. Nat Genet 20:78–82

Yoshikawa DK, Kollar EJ (1981) Recombination experiments on the odontogenic roles of mouse dental papilla and dental sac tissues in ocular grafts. Arch Oral Biol 26:303–307

Cell Tissue Res (2008) 331:461–472
DOI 10.1007/s00441-007-0528-x

REGULAR ARTICLE

Characteristic phenotype of immortalized periodontal cells isolated from a Marfan syndrome type I patient

Momotoshi Shiga · Masahiro Saito · Mitsu Hattori · Chiharu Torii · Kenjiro Kosaki · Tohru Kiyono · Naoto Suda

Received: 17 May 2007 / Accepted: 20 September 2007 / Published online: 30 November 2007

Abstract The periodontal ligament (PDL) is situated between the tooth root and alveolar bone, thereby supporting the tooth, and is composed of collagen and elastic system fibers. Marfan syndrome type I (MFS1, MIM #154700) is caused by mutations in *FBN1* encoding fibrillin-1, which is a major microfibrillar protein of elastic system fibers. MFS1 is characterized by tall stature, aortic/mitral valve prolapse, and ectopia lentis and is occasionally accompanied by severe periodontitis. Since little is known about the biological functions of elastic system fibers in PDLs and the pathogenesis of the periodontitis in MFS1, PDL cells were isolated from an MFS1 patient with a heterozygous missense mutation in a calcium-binding epidermal-growth-factor-like domain of *FBN1*. Isolated PDL cells were immortalized by transducing a retrovirus carrying genes for the human Polycomb group protein, Bmi-1, and human telomerase reverse transcriptase. Immortalized PDL cells from the MFS1 patient (termed M-HPL1) and those of a healthy volunteer (termed HPDL2) both expressed various PDL-related genes. The growth and attachment of M-HPL1 and HPDL2 to hydroxyapatite particles were comparable. However, when M-HPL1 were transplanted with hydroxyapatite particles into immunodeficient mice, disorganized cell alignment and irregular microfibril assembly were noted. The activation of the signaling of transforming grwoth factor-β (TGF-β) is thought to cause the pathogenesis for lung and cardiovascular abnormalities in MFS1. Interestingly, M-HPL1 shows a higher level of activated TGF-β than HPDL2. Thus, M-HPL1 represent a powerful tool for clarifying the biological roles of elastic system fibers in PDL and the pathogenesis of periodontitis in MFS1. Our findings also suggest that *FBN1* regulates cell alignment and microfibril assembly in PDLs.

Keywords Elastic fiber · Fibrillin-1 · Marfan syndrome · Periodontitis · Periodontal ligament · Human

This work was supported by Grants-in-Aid (16390604, 16659570, and 18390552) for Scientific Research from the Ministry of Education, Culture, Sports, Science, and Technology of Japan.

M. Shiga · M. Hattori · N. Suda (✉)
Maxillofacial Orthognathics, Department of Maxillofacial Reconstruction and Function,
Division of Maxillofacial/Neck Reconstruction, Graduate School, Tokyo Medical and Dental University,
1-5-45 Yushima, Bunkyo-ku,
Tokyo 113-8549, Japan
e-mail: n-suda.mort@tmd.ac.jp

M. Saito
Department of Molecular and Cellular Biochemistry, Graduate School of Dentistry, Osaka University,
Osaka 565-0871, Japan

C. Torii · K. Kosaki
Department of Pediatrics, Keio University School of Medicine,
Tokyo 160-8582, Japan

T. Kiyono
Virology Division, National Cancer Center Research Institute,
Tokyo 104-0045, Japan

Introduction

The periodontal ligament (PDL) is a specialized connective tissue situated between the cementum covering the root of teeth and the alveolar bone socket (Beertsen et al. 1997; Freeman 1998). PDLs consist of various kinds of cells and fibers. The cells include fibroblasts, epithelial cell remnants of Malassez, macrophages, undifferentiated mesenchymal cells, cementoblasts, osteoblasts, and osteoclasts. The fibers include collagen and elastic system fibers. PDLs are well adapted to support teeth in bone and to act as a sensory

receptor. To support teeth, collagen fibers are embedded both in the cementum and alveolar bone, and each collagen fiber works as a spliced rope to withstand the considerable forces of mastication.

Elastic system fibers provide elasticity and resistance to stretch and expansion forces (Mecham 1991). They are widely distributed in various tissues, e.g., skin, lungs, eyes, and blood vessels. Three types of elastic system fibers (oxytalan and elastic and elaunin fibers) are known; they differ in the content of elastin (Kielty et al. 2002). Oxytalan fibers solely consist of bundles of microfibrils, which are predominantly composed of glycoproteins and fibrillin-1 and -2. The elastic fibers are constructed of bundles of microfibrils peripherally associated with elastin. In the elaunin fibers, bundles of microfibrils are intermingled with small amounts of elastin. In the PDL, the main elastic system fibers are oxytalan fibers oriented in an occluso-apical direction (Fullmer et al. 1974; Beertsen et al. 1997). A small amount of elaunin fibers is also found in the apical region (Staszyk and Gasse 2004; Sawada et al. 2006). In contrast to collagen fibers, the biological functions of the elastic system fibers in PDLs are still obscure.

Marfan syndrome type I (MFS1, MIM #154700) is an autosomal dominant disorder affecting the elastic system fibers. Its prevalence has been estimated to be 2–3 per 10,000 (Nollen and Mulder 2004). MFS1 is characterized by various clinical manifestations primarily in skeletal, ocular, and cardiovascular organs, e.g., tall stature, aortic dissection, mitral valve prolapse, and ectopia lentis (Pyeritz 2000). The responsible gene for this syndrome has been identified as *FBN1*, which encodes the major microfibrillar protein, fibrillin-1 (Dietz et al. 1991; Maslen et al. 1991). In addition to anomalies in skeletal, ocular, and cardiovascular systems, MFS1 exhibits characteristic oral features including maxillary protrusion (Westling et al. 1998), high palate, and crowding and fragility of the temporomandibular joint (Bauss et al. 2004). Severe periodontitis, which has a serious impact on the quality of life of MFS1 patients, is occasionally associated with this syndrome (Straub et al. 2002).

To clarify the biological functions of fibrillin-1 in PDLs and the pathogenesis of the periodontitis in MFS1, PDL cells have been isolated from an MFS1 patient. The prepared immortalized PDL cells, which have a mutation in a calcium-binding epidermal-growth-factor-like (cbEGF) domain of fibrillin-1, might be a powerful tool to help answer these questions.

Materials and methods

Subjects

The patient was a 46-year-old female. She was 172 cm tall, weighed 58 kg, and had arachnodactyly. Her father and younger brother were also diagnosed as having Marfan syndrome. She had previously had dissecting aneurysm of the aorta and had had a surgical replacement of the aortic root (Bentall operation) at 42 years of age. She had suffered from mitral valve prolapse and had had a replacement of the mitral valve at 46 years of age. Since she had severe periodontitis in all teeth, all teeth were extracted before the mitral valve replacement to avoid infective endocarditis. The patient kindly provided these teeth to us with consent.

Extracted teeth were also provided by three healthy volunteers (volunteer A, 15-year-old male; volunteer B, 15-year-old male; volunteer C, 21-year-old female) during the course of orthodontic treatment, with consent. The experimental protocol was approved by the Ethical Review Committee of Tokyo Medical and Dental University.

Isolation and culture of primary PDL cells

Isolation and culture of human PDL cells were performed as previously described (Kapila et al. 1996; Shiga et al. 2003). In brief, the extracted teeth from the MFS1 patient and healthy volunteers were washed with α-minimum essential medium (α–MEM; Kohojin Bio, Japan) containing Antibiotic-Antimycotic (GIBCO, Calif.). The PDL attached to the middle part of the root was isolated with a surgical scalpel. The PDL was minced and placed in 35-mm tissue culture dishes (SUMILON, Japan). The explants were then covered with sterile glass coverslips and incubated in α–MEM with 10% fetal bovine serum (FBS; Japan Bioserum, Japan) at 37°C under 5% CO_2 and 95% air until cells outgrew from the explants. After the outgrowth of cells, coverslips were removed from the culture dishes. The culture medium was changed every 3 days. PDL cells from passages 3–7 were used for examing mineralization, measuring alkaline phosphatase (ALP) activity, and transduction.

Mineralization of the primary culture of PDL cells

To determine the mineralization of cultured PDL cells, cells were plated at 2.0×10^4 cells/cm^2 and cultured in α–MEM containing 10% FBS. After cells became confluent, the medium was changed to α–MEM containing 10% FBS with 50 μg/ml ascorbic acid (Wako, Japan), 10 nM dexamethasone (Sigma, Mo.), and 10 mM β-glycerophosphate (Sigma) in some cultures, as previously described (Cho et al. 1992; Nohutcu et al. 1997; Chien et al. 1999). The medium was changed every 3 days, and the cells were cultured for 3 weeks. Mineralized matrix in the culture were stained by Alizarin Red S (Wako, Japan) at the end of the culture (Saito et al. 2002). All experiments were performed in triplicate wells.

ALP activity

Cells were cultured under the same conditions as described above for mineralization. ALP activity was assayed in cell lysates by enzymatic conversion of the p-nitrophenylphosphate substrate to p-nitrophenol by using the LabAssay ALP kit (Wako) according to the manufacturer's instructions. The activity was recorded as millimoles per milligram per 15 min. The total protein amount in the cell lysates was measured by using the Bradford microassay (Bio-Rad, Calif.) according to the manufacturer's instructions.

Immunohistochemical staining of cultured PDL cells

Cultured PDL cells were immunohistochemically stained by using anti-human periostin rabbit polyclonal antibody (BioVendor laboratory Medicine, N.C.), anti-bovine collagen type XII monoclonal antibody (Clone 378D5, Kamiya Biomedical, Wash.), anti-active transforming growth factor-β (TGF-β) rabbit polyclonal antibody (LC1-30, provided by K. Flanders, National Cancer Institute, Md.; Flanders et al. 1989), or anti-human latency-associated peptide-β1 (LAP-β1) goat polyclonal antibody (R&D systems, Minn.). Cells (2.0×10^4 cells/cm^2) were cultured on poly-L-lysine-coated glass (Iwaki, Japan). They were then fixed with 4% paraformaldehyde (PFA) for 30 min, blocked with 1% bovine serum albumin (BSA), and incubated with each antibody for 1 h. Sections were then treated with Alexa Fluor 594 goat anti-rabbit IG (H+L; Invitrogen, Calif.), Alexa Fluor 488 goat anti-mouse IG (H+L; Invitrogen), or Alexa Fluor 488 donkey anti-goat IG (H+L; Invitrogen). As negative controls, primary antibodies were replaced with normal rabbit serum (Vector Laboratories, Calif.), mouse IgG (Jackson Immuno Research Laboratories, Pa.), or normal goat serum (Vector Laboratories). After washes with phosphate-buffered saline, fluorescence was observed by means of a fluorescence microscope (AF6000, Leica, Germany).

Mutational analysis

DNA from the MFS1 patient and healthy volunteers was extracted by using a DNA extraction kit (Bio-Rad, Calif.). Extracted DNA was amplified by using specific primers for *FBN1* and *TGFBR2* (encoding TGF-β receptor II, which is the responsible gene for Marfan syndrome type II; MFS2, MIM #154705; Mizuguchi et al. 2004). Primer sequences and polymerase chain reaction (PCR) conditions were as given on the website of "Multiple Malformation Syndromes (http://www.dhplc.jp/genetics/frame.html)" provided by the Department of Pediatrics, Division of Medical Genetics, Keio University School of Medicine. Mutations in each amplicon were analyzed by denaturing high-performance liquid chromatography (DHPLC), as described in previous studies (Kosaki et al. 2005; Udaka et al. 2005).

After DHPLC analysis, PCR products were purified on a desalting column and were sequenced by a dideoxy-sequencing method (BigDye Dideoxy sequencing kit, Applied BioSystems, Calif.) and an automated sequencer (ABI3100, Applied Biosystems; Udaka et al. 2005).

Retroviral vectors and infection

Primary PDL cells, obtained from a healthy volunteer and the MFS1 patient, were transduced with genes for human Polycomb group protein, Bmi-1, and human telomerase reverse transcriptase (hTERT) by using retrovirus-mediated gene transfer. The production and infection of LXSN-Bmi-1 and MSCVpuro-hTERT retroviruses were performed as described previously (Kyo et al. 2003; Saito et al. 2005). The infected cells were selected in the presence of geneticin (125 μg/ml) or puromycin (0.5 μg/ml). For combined retroviral infection, cells were sequentially transduced with LXSN-Bmi-1 and then with MSCVpuro-hTERT. Stably transduced cells were maintained in the medium described above.

Detection of telomerase activity

After infection, telomerase activity was determined by a telomerase repeat amplification assay by using the TRA-Peze Telomerase Detection Kit (CHEMICON International, Calif.), according to the manufacturer's instructions.

Cell proliferation in monolayer culture

To examine cell proliferation, cells were inoculated at 5.0×10^3 cells/cm^2 into 6-well dishes (Iwaki, Japan) and cultured in α–MEM containing 10% FBS. The medium was changed every 3 days, and cells were counted every 3 days up to day 15. All experiments were performed in triplicate wells.

Western blot analysis

The introduction of Bmi-1 was identified by Western blot analysis by using anti-human Bmi-1 monoclonal antibody (BD Pharmingen, San Diego, Calif.). Cells were cultured in α–MEM containing 10% FBS and lysed in buffer containing 50 mM TRIS-HCl (pH 7.4), 125 mM NaCl, 0.1% Nonident P-40 (NP-40; Sigma), and 1 mM each of EDTA and phenylmethylsulfonyl fluoride, followed by sonication. After electrophoretic resolution of the cell lysate (20 μg each protein) on 12.5% SDS-polyacrylamide gels, the proteins were transferred to polyvinylidene difluoride (PVDF) membranes (Amersham, N.J.). The subsequent